

Pacific Northwest National Laboratory

Operated by Battelle for the
U.S. Department of Energy

Colloid Suspension Stability and Transport Through Unsaturated Porous Media

M. A. McGraw
D. I. Kaplan

RECEIVED
MAY 27 1997
OSTI

April 1997

Prepared for the U.S. Department of Energy
under Contract DE-AC06-76RLO 1830

MASTER

PNNL-11565

DISCLAIMER

This report was prepared as an account of work sponsored by an agency of the United States Government. Neither the United States Government nor any agency thereof, nor Battelle Memorial Institute, nor any of their employees, makes any warranty, express or implied, or assumes any legal liability or responsibility for the accuracy, completeness, or usefulness of any information, apparatus, product, or process disclosed, or represents that its use would not infringe privately owned rights. Reference herein to any specific commercial product, process, or service by trade name, trademark, manufacturer, or otherwise does not necessarily constitute or imply its endorsement, recommendation, or favoring by the United States Government or any agency thereof, or Battelle Memorial Institute. The views and opinions of authors expressed herein do not necessarily state or reflect those of the United States Government or any agency thereof.

PACIFIC NORTHWEST NATIONAL LABORATORY
operated by
BATTELLE
for the
UNITED STATES DEPARTMENT OF ENERGY
under Contract DE-AC06-76RLO 1830

Printed in the United States of America

Available to DOE and DOE contractors from the
Office of Scientific and Technical Information, P.O. Box 62, Oak Ridge, TN 37831;
prices available from (615) 576-8401.

Available to the public from the National Technical Information Service,
U.S. Department of Commerce, 5285 Port Royal Rd., Springfield, VA 22161



This document was printed on recycled paper.

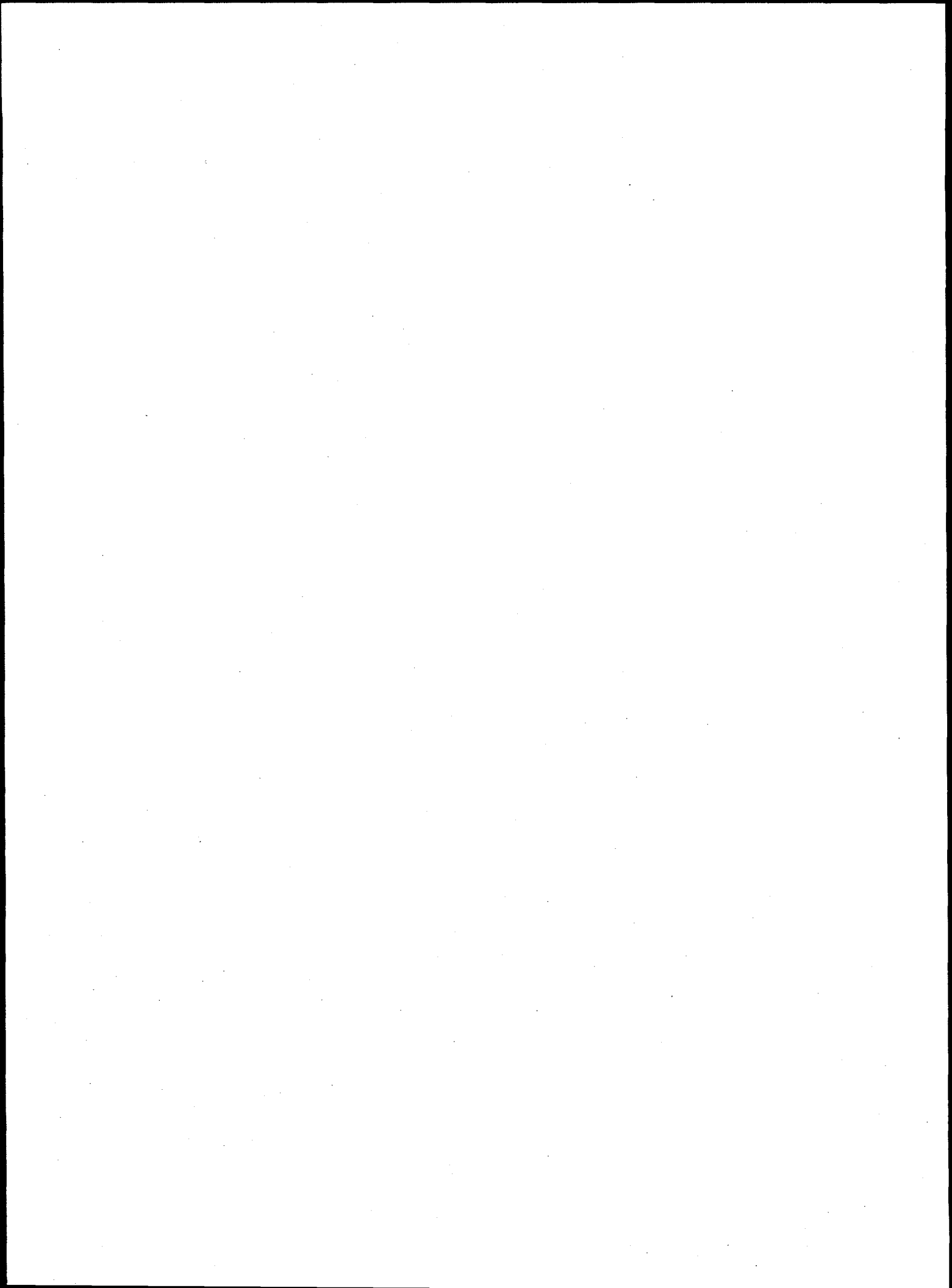
Colloid Suspension Stability and Transport Through Unsaturated Porous Media

M. A. McGraw
D. I. Kaplan

April 1997

Prepared for the U. S. Department of Energy
under Contract DC-AC06-76RLO 1830

Pacific Northwest National Laboratory
Richland, Washington 99352



Executive Summary

Contaminant transport is traditionally modeled in a two-phase system: a mobile aqueous phase and an immobile solid phase. Over the last 15 years, there has been an increasing awareness of a third, mobile solid phase. This mobile solid phase, or mobile colloids, are organic or inorganic submicron-sized particles that move with groundwater flow. When colloids are present, the net effect on radionuclide transport is that radionuclides can move faster through the system. It is not known whether mobile colloids exist in the subsurface environment of the Hanford Site. Furthermore, it is not known if mobile colloids would likely exist in a plume emanating from a Low Level Waste (LLW) disposal site. No attempt was made in this study to ascertain whether colloids would form. Instead, experiments and calculations were conducted to evaluate the likelihood that colloids, if formed, would remain in suspension and move through saturated and unsaturated sediments.

The objectives of this study were to evaluate three aspects of colloid-facilitated transport of radionuclides as they specifically relate to the LLW Performance Assessment. These objectives were: 1) determine if the chemical conditions likely to exist in the near and far field of the proposed disposal site are prone to induce flocculation (settling of colloids from suspension) or dispersion of naturally occurring Hanford colloids, 2) identify the important mechanisms likely involved in the removal of colloids from a Hanford sediment, and 3) determine if colloids can move through unsaturated porous media.

Mobile colloid formation is commonly described as a three-step process: genesis, stabilization, and transport. Colloid genesis describes how the micron-sized particles are formed in groundwater. Stabilization describes how the colloids are brought into suspension, which is a function of the colloid and groundwater chemical composition and water flow (kinetic) forces. Transport describes how the suspended colloid move through the porous media or are retained by the porous media by physical forces (such as diffusion, straining, or gravitation settling) or physicochemical attraction of the colloid to the matrix.

As the second step in mobile colloid formation indicates, colloids must remain in suspension, i.e., not flocculate, in order to be transported with groundwater flow. A series of batch experiments was conducted to identify the chemical conditions where dispersion and flocculation (settling out of suspension) of Hanford sediment colloids (<1000 nm) would occur. These experiments determined the critical flocculation concentration (CFC), the minimum electrolyte concentration to induce colloids to flocculate from suspension. The CFC values were calculated for a range of sodium concentrations and pH values that may exist in the near and far fields. These two groundwater parameters are considered to be among the most important parameters affecting colloid suspension stability. The experiments suggest that natural Hanford groundwaters are not likely to maintain colloids in suspension. This in turn suggests that little or no mobile colloids are likely to exist in natural Hanford sediments. Specifically, the groundwater electrolyte concentration (9.86 mmol/L) is sufficiently high for the relatively low sodium concentrations (sodium adsorption ratio [SAR] = 1.04) and pH (8.1) conditions existing in Hanford groundwaters to induce colloid flocculation. Chemical conditions in the near field also are not likely to be conducive for maintaining colloids in suspension. Based on these experiments, even fewer suspended colloids are predicted to exist in the near field than in the far field.

Simulations were conducted of colloid removal by saturated porous media. These simulations were based on filtration theory, a semi-empirical model that explicitly attributes colloid removal to diffusion (Brownian motion), electrostatic attraction (colloid/colloid and colloid/sediment), gravitational settling, and interception (sieving). These simulations indicated that colloids with diameters between 200 and 500 nm were the most likely to move through sandy-textured sediments. Below this range, colloids were removed from suspension by diffusional, followed by adsorption,

processes. Above this range, colloids were removed from suspension by gravitational settling. Mobile colloid sizes reported in the literature are essentially always in this size range, providing additional credence to these results. One important implication of this finding is that even if a suspension of nanometer-sized colloids were formed from the waste form (such as colloidal radionuclide precipitates), they would likely be retained by the sediment as a result of diffusional removal processes. These simulations also indicate that colloid removal by sediments was not sensitive to flow rate, but was sensitive to colloid size and sediment particle size.

Experiments were also conducted to determine if colloids could move through unsaturated conditions. This issue is experimentally difficult to evaluate. The approach taken in this series of studies was to use an extremely well controlled and defined system. The system consisted of water, uniformly sized sand, and fluorescent latex colloids. The degree of saturation in the sand columns was carefully controlled using an unsaturated flow apparatus (UFA). The effect of colloid size (from 52 to 1900 nm) and degree of saturation (from 6 to 100%) on colloid transport were investigated. These experiments simulated a system in which colloids were already formed and were highly dispersive (would not flocculate from suspension). Under saturated conditions, the amount of colloids removed from suspension did not vary as a function of colloid size. However, in unsaturated conditions, colloid size had a profound effect on colloid transport. At 6% volumetric water content, approximately the degree of saturation expected in the Hanford vadose zone, colloid removal increased exponentially as colloid size increased. It was proposed that the decrease in colloid mobility at low volumetric contents was due to the colloids being dragged along the sand grain and retarded as the ratio between the water film thickness and colloid size decreased. The most mobile colloids at 6% water content were less than 60 nm.

In conclusion, these studies suggest that if colloids containing radionuclides (radiocolloids) are present, the groundwater chemistry in the near and far fields likely will cause them to flocculate. This would preclude colloid-facilitated transport of radionuclides from the disposal site. In the event that radiocolloids are in fact stable in groundwater, only the smallest of colloids, <60 nm in diameter, would be able to move through the unsaturated vadose zone. The larger colloids would be retained by the sediment. If these <60-nm radionuclides reached the aquifer, they likely would be removed from the groundwater by diffusional processes.

DISCLAIMER

**Portions of this document may be illegible
in electronic image products. Images are
produced from the best available original
document.**

Contents

Executive Summary.....	iii
Symbols and Acronyms.....	x
1.0 Introduction.....	1.1
1.1 Literature Review.....	1.1
1.1.1 Formation Of Groundwater Mobile Colloids.....	1.1
1.1.2 Colloids In Natural Systems.....	1.3
1.1.3 Non-Radioactive Contaminant Transport With Colloids.....	1.4
1.1.4 Radioactive Contaminant Transport With Mobile Colloids.....	1.4
1.1.5 Colloid Mobility Under Saturated Conditions.....	1.5
1.1.6 Colloid Mobility Under Unsaturated Conditions.....	1.6
1.2 Objectives.....	1.7
1.3 Scope.....	1.7
2.0 Suspension Stability of Colloids Collected From Hanford Sediments as a Function of pH and Sodium Concentrations.....	2.1
2.1 Materials and Methods.....	2.1
2.2 Results and Discussions.....	2.2
3.0 Colloid Transport Through Saturated Systems.....	3.1
3.1 Theory.....	3.1
3.2 Results and Discussions.....	3.3
4.0 Effect of Colloid Size and Degree of Saturation on Colloid Transport.....	4.1
4.1 Materials.....	4.1
4.1.1 Sand Characterization.....	4.1
4.1.2 Colloid Quantification.....	4.3
4.1.3 Colloid Hydrophobicity Measurements.....	4.5
4.1.4 Colloid Zeta Potentials.....	4.6
4.2 UFA/Colloid Transport.....	4.7
4.2.1 Saturated Column Experiments.....	4.7
4.2.2 Unsaturated Column Experiments.....	4.8

4.2.3 Test of UFA for Colloid Transport.....	4.15
4.3 Effect of Particle Size on Colloid Transport.....	4.19
4.3.1 Saturated Column Experiments.....	4.21
4.3.2 Unsaturated Column Experiments.....	4.22
4.3.3 Discussion.....	4.25
5.0 Conclusion	5.1
6.0 References	6.1
Appendix-A	A.1
Appendix-B.....	B.1

Figures

1.1 Three-Step Process for the Generation of Groundwater Mobile Colloids.....	1.2
2.1 Critical Flocculation Concentrations (CFC) of Suspension of the <1000-nm Fraction of a Hanford Sediment (Trench AE-3) as a Function of pH and Na:Ca Molar Ratios.....	2.2
2.2 Experimentally Derived Critical Flocculation Concentrations (CFC) of Hanford Sediment Colloids (<1000 nm) as a Function of Sodium Adsorption Ratio and pH.....	2.3
2.3 Experimentally Derived Critical Flocculation Concentrations (CFC) of Hanford Sediment Colloids (<1000 nm) in Sodium Solutions (SAR = infinity) as a Function of pH.....	2.4
3.1 Effect of Groundwater Flow Rate on Single-Collector Efficiency (Equations 3.2, 3.3, and 3.4).....	3.4
3.2 Effect of Media Particle (Sediment) Diameter on Single-Collector Efficiency (Equations 3.2, 3.33, and 3.4).....	3.4
3.3 Effect of Mobile Colloid Diameter on Single-Collector Efficiency (Equations 3.2, 3.3, and 3.4).....	3.5
3.4. Relationship Between Total Single-Collector Efficiency and Removal Efficiency Factor (Equations 3.5 and 3.6).....	3.5
4.1 SEM Image of Quartz.....	4.1
4.2 SEM Image of Feldspar.....	4.2
4.3 SEM Image of Mica.....	4.2
4.4 Emission Spectra of the 189-nm Colloids at Different Concentrations.....	4.4
4.5 Calibration Curve for the 189-nm Colloids (Ex = 423 nm, Em = 470 nm).....	4.5
4.6 Effect of Contact Angle on the Degree of Particle Immersion at the Air-Water Interface...	4.6
4.7 Schematic of UFA Rotor.....	4.9
4.8 Schematic of UFA Face Seal.....	4.10
4.9 The Variability of the Volumetric Water Content Between the 90 Repacked Sand Columns Used in This Study.....	4.13
4.10 The Variability of the Hydraulic Conductivity Between the 90 Repacked Sand Columns Used in This Study.....	4.14
4.11 Breakthrough Curve of 10^{-3} M KBr at Different Flow Rates and Rotation Speeds to Determine if Changes in Rotation Speed Enhance Transport.....	4.17

4.12 The Breakthrough of 189-nm Colloids at Different Flow Rates and Rotation Speeds to Determine if Changes in the Rotation Speed Enhances the Transport of Colloids.....	4.18
4.13 The Concentration Breakthrough of 189-nm Colloids Used in ANOVA Analysis to Test whether the Rotation Speed Affects Colloid Transport.	4.18
4.14 Possible Retention Sites for Mobile Colloids Through Porous Media Under Partially Saturated Conditions.....	4.19
4.15 Cumulative Mass Recovery of 189-nm Colloids From the Column That was Used for Coefficient of Variation Analysis to Test if the Rotation Speed Affects Colloid Transport.	4.20
4.16 The Effect of Colloid Size on the Average Breakthrough of KBr and Latex Colloids Without Surface Functional Groups From Duplicate Experiments Under Saturated Conditions.....	4.20
4.17 The Effect of Colloid Size on the Cumulative Mass Recovered for KBr and Latex Colloids Without Surface Functional Groups From Duplicate Experiments Under Saturated Conditions.....	4.22
4.18 The breakthrough of KBr and Latex Colloids Without Surface Functional Groups at $\theta_{avg} = 6\%$ to Examine the Effect of Size on Colloid Mobility.....	4.23
4.19 Cumulative Mass Recovered at 50 Pore Volumes for Latex Colloids Without Surface Functional Groups as a Function of Size at $\theta_{avg} = 6\%$	4.23
4.20 Proportional Schematic of Different Sized Colloids Without Surface Functional Groups in a 114-nm Water Film ($\theta_{avg} = 6\%$).....	4.24
4.21 Cumulative Mass Recovery at 50 Pore Volumes for Latex Colloids Without Surface Functional Groups as a Ratio of the Water Film Thickness/Colloid Size.....	4.25
A.1 Emission Spectra of the 52-nm Colloids at Different Concentrations.....	A.2
A.2 Calibration Curve for the 52-nm Colloids (Ex = 440 nm, Em = 489 nm).....	A.2
A.3 First Emission Spectra of the 545-nm Colloids at Different Concentrations.....	A.3
A.4 First Calibration Curve for the 545-nm Colloids (Ex = 440 nm, Em = 485 nm).....	A.3
A.5 Emission Spectra of the 545-nm Colloids at Different Concentrations After Maintenance.....	A.4
A.6 Calibration Curve for the 545-nm Colloids After Maintenance (Ex = 440 nm, Em = 485 nm).....	A.4
A.7 Emission Spectra of the 910-nm Colloids at Different Concentrations.....	A.5
A.8 Calibration Curve for the 910-nm Colloids (Ex = 490 nm, Em = 518 nm).....	A.5
A.9 Emission Spectra of the 1900-nm Colloids at Different Concentrations.....	A.6
A.10 Calibration Curve for the 1900-nm Colloids (Ex = 468 nm, Em = 536 nm).....	A.6

Tables

2.1	Chemical Composition of an Uncontaminated Hanford Groundwater (Well: 6-S3-25 from 1985 to 1990) and Estimated Plume Concentrations in the Near Field.....	2.3
3.1	Default Values Used in Calculations of Colloid Filtration by Porous Media in a Saturated System	3.3
4.1	Fluorescent Properties of Colloids.....	4.4
4.2	Relative Colloid Contact Angles (Average of 5-10 Replicates).....	4.6
4.3	Average of Two Zeta Potential Measurements for Latex Colloids and AZ55 Standards	4.7
4.4	Comparison of the Stokes Sedimentation Velocity and Specific Discharge for the Colloid Experiments	4.16
B.1	Averaged Volumetric Water Content, Hydraulic Conductivity, and Standard Deviations.	B.1

Symbols and Acronyms

a	burette cross sectional area (cm ²)
A	sample cross-sectional area (cm ²)
A _{ss}	specific surface area (cm ² /g)
d _c	colloid diameter (nm)
d _m	mean grain size (μm)
d ₀	molecular diffusion coefficient
H ₁	initial water column height (cm)
H ₂	final water column height (cm)
k	Boltzman's constant
K	hydraulic conductivity (cm/sec)
L	sample length (cm)
n	porosity
N	Avogadro's number
q	fluid flux (cm/s)
r	distance from axis of rotation (cm)
r _d	radius of diffusing molecule (m)
R	gas constant (J/K·mol)
R _c	Reynolds number
t	time for water to fall from H ₁ to H ₂ (sec)
t _w	water film thickness (nm)
T	temperature (K)
U _∞	approach velocity (cm/s)
φ	contact angle
η	single collector efficiency
η _D	single collector efficiency - diffusion
η _G	single collector efficiency - gravitational sedimentation
η _I	single collector efficiency - interception
λ ₀	clean bed filter coefficient (m ⁻¹)
μ	viscosity (kg·m/s)
v ₀	water velocity (cm/s)
θ _s	saturation
θ	volumetric water content
ρ	density (g/cm ³)
ρ _b	bulk density (g/cm ³)
ρ _{sand}	density of sand (g/cm ³)
ρ _{sp}	density of suspended particle (g/cm ³)
ρ _w	density of water (g/cm ³)
σ	surface charge density (μC/cm ²)
v	specific discharge (cm/s)
ω	rotation speed (1/s)
ψ	matric potential
ζ	zeta potential (mV)
[C/C ₀]	normalized concentration breakthrough
[M/M ₀]	cumulative percent mass recovered
CFC	Critical Flocculation Concentration (mmol/L)
NOM	Natural Organic Matter

DOC	Dissolved Organic Carbon
LLW	Low Level Waste
PA	Performance Assessment
SAR	Sodium Adsorption Ratio (mmol/L) ^{0.5}
UFA	Unsaturated Flow Apparatus

1.0 Introduction

The mobility of radionuclides through porous media may be enhanced by colloidal material such as clays, silicates, iron oxides, bacteria, viruses, and humic acids. Therefore, it is important to understand the mechanisms that control colloid mobility. Recent studies have focused on saturated colloid transport, and it is not clear if colloids can move under partially saturated conditions. One reason that transport under partially saturated conditions may be less important is that the effective pore size through which the colloids move is reduced as the volumetric water content decreases. However, if colloids are mobile under partially saturated conditions, it is important to understand the mechanisms that influence their mobility. This will affect the subsequent modeling of contaminant transport.

1.1 Literature Review

The stability and migration of colloidal particles in the subsurface are affected by changes in ionic strength, fluid velocity, electrochemical processes, soil pH, or combinations of these factors (Greene et al. 1994, Puls et al. 1993). The release of fines has been studied extensively in the petroleum industry because mobile colloids can decrease formation permeability and hence its productivity (Sharma and Yortsos 1987, Kia et al. 1987). In the agriculture industry, the dispersion of clays is important because it can adversely affect the soil permeability, water infiltration, soil erosion, and the formation of aggregates (Miller et al. 1990, Goldberg and Foster 1990, Frenkel et al. 1978, Bertrand and Sor 1962).

In the last 15 years, a new focus has developed that examines whether colloidal particles can serve as a vector for contaminant transport in the subsurface (Ryan and Elimelech 1996, McCarthy and Zachara 1989, McDowell-Boyer et al. 1986). In this context, the mechanisms that control subsurface colloid retention and mobility are important. The filtration of colloids has been studied for wastewater treatment (Tien 1989, Yao et al. 1971, Herzig et al. 1970). However, the focus has been on the removal of colloids rather than their mobility.

1.1.1 Formation of Groundwater Mobile Colloids

Mobile colloids are organic or inorganic, micron-sized particles that move with the flow of groundwater. The formation of mobile groundwater colloids is commonly described as requiring three steps: genesis, stabilization, and transport (McDowell-Boyer et al. 1986, McCarthy and Zachara 1989) (Figure 1.1). Colloid genesis describes how micron-sized particles are formed in the groundwater. Four mechanisms of colloid genesis have been identified. The first mechanism is the translocation of colloids from the overlying vadose or soil layer into the groundwater (McDowell-Boyer et al. 1986, Kaplan et al. 1993, 1996c, 1997). This is a well-known process in soil pedogenesis and is responsible for the formation of different strata in soils (Birkeland 1984). Colloid genesis can also occur when cementing agents, such as iron oxides (Schwertmann and Taylor 1989, Ryan and Gschwend 1990) and calcium carbonates (Ronen et al. 1992), are dissolved, thereby releasing otherwise stationary particles into the mobile phase. The reductive dissolution of iron oxide cements appears to be a second mechanism by which colloids can be mobilized in natural waters or in contaminant plumes containing levels of dissolved organic carbon high enough to promote microbial activity and anoxic conditions. The dissolution of iron oxides in oxide-cemented sand under anoxic conditions liberated layer silicate clays previously bound to the aquifer matrix (Ryan and Gschwend 1990). Similarly, siliceous colloidal material is released into groundwater in a calcareous environment because infiltration of water of different composition dissolve carbonate cements (McCarthy and Zachara 1989).

Colloids in Groundwater

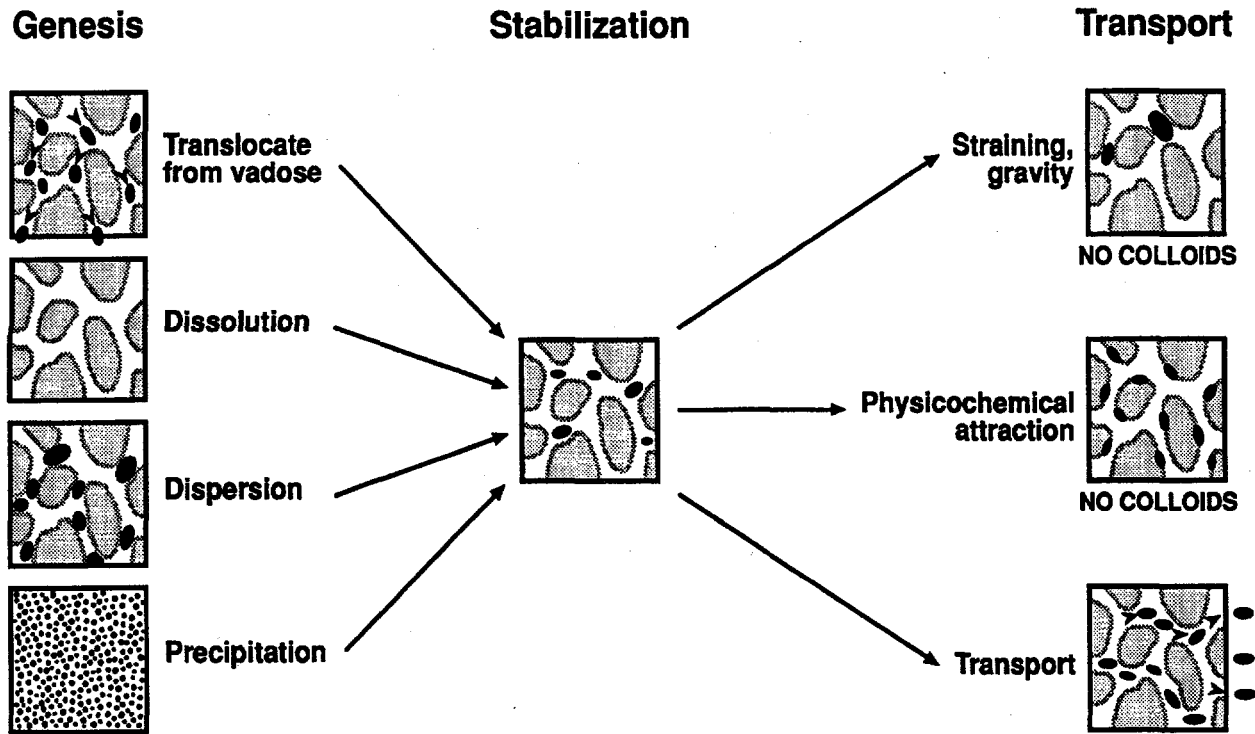


Figure 1.1. Three-Step Process for the Generation of Groundwater Mobile Colloids

A third mechanism for colloid genesis is the dispersion of fine particles within the aquifer matrix into the aqueous phase. This usually occurs as a result of decreasing the electrolyte concentration of the groundwater or shifting the ion balance from one dominated by calcium to one dominated by sodium. The net effect of both changes in groundwater chemistry is an increase in the repulsive forces between particles and an increase in the propensity for the colloids to remain in suspension. This has been a particularly important mechanism of colloid genesis in areas of California where aquifers are recharged with rainwater of low electrolyte concentration (Nightingale and Bianchi 1977). The fourth mechanism of colloid genesis is precipitation. Colloidal precipitates can form in the aqueous phase in natural and especially in altered hydrologic systems, where changes in geochemistry induce supersaturation with respect to solid phases that can readily precipitate (Ho and Miller 1986, Gschwend and Reynolds 1987). Geochemical gradients are common between contaminant plumes and associated uncontaminated groundwaters. As an example, Gschwend and Reynolds (1987) observed the precipitation of ferrous phosphate solids in groundwater beneath a sewage infiltration basin. Also, iron oxide colloids have been observed to precipitate in groundwater as a result of both pH changes and oxygenation (Schwertmann and Taylor 1989).

The second step in mobile colloid formation following colloid genesis is stabilization (Figure 1.1). Once colloids are formed, they must remain in suspension; otherwise, the particles settle out of solution and do not move through the aquifer. Groundwater chemistry and flow rates control colloid stability. Whether a colloid will remain in suspension, flocculate, or be retained by the sediment depends on a complex combination of colloid, sediment, and groundwater factors. The complicated interdependency of these factors makes it difficult to predict particle behavior, based on current understanding and models (Tien 1989, van Olphen 1977). However, general concepts are well-established for assessing these interactions qualitatively. Laboratory studies have demonstrated a three-way interaction of dissolved sodium concentration, pH, and ionic strength on

colloid stability (Suarez et al. 1984, Kaplan et al. 1996c). This interaction is predicted by electrical double-layer theory in which repulsive forces between expanding double layers increase as ionic strength decreases and dissolved sodium concentrations and pH increase (van Olphen 1977). Laboratory studies have provided valuable information regarding mechanisms governing clay dispersions; however, they have had only limited success in providing values that are directly relevant to field conditions. Not surprising, the groundwater flow rate also has a profound effect on maintaining colloids in suspension (Kaplan et al. 1993). As flow rate changes, not only does the concentration of colloids released from a system change, but several properties of the colloids also change (Kaplan et al. 1993). For instance, Kaplan et al. (1993) reported that as colloid flow rate increased, the mean colloid size increased, and the surface charge of the colloids decreased. The increase in colloid size was attributed to the higher flow rate providing greater kinetic energy into the system, thereby providing sufficient energy (shear) to maintain the larger particles in suspension. The decrease in colloid surface charge was attributed to the fact that, at low flow rates, only the colloids of highest charge could remain in suspension. At higher flow rates, less charge was needed to keep the colloids in suspension because kinetic energy was present to maintain the colloids in suspension.

The last step in mobile colloid formation is the transport of the suspended colloid through the porous media (Figure 1.1). Even if the radionuclides are formed and then suspended in solution, they will pose little health threat if they do not move with the groundwater flow. Transport of suspended colloid occurs when colloid retention forces such as straining, gravitation settling, or physicochemical sorption to the immobile porous media do not occur. Colloid transport through porous media has been studied extensively for wastewater treatment processes (see references in Tien 1989). Models developed from these studies conducted primarily in the 1970s are being modified for groundwater colloid transport problems. One of the main obstacles in applying these semi-mechanistic models for groundwater transport is that they describe the transport of uncharged colloids through well-defined, homogeneous media (O'Melia 1987) while omitting the transport of naturally occurring charged colloids through heterogeneous media.

1.1.2 Colloids in Natural Systems

The most extensive review of natural colloids was done by McCarthy and Degueudre (1993). The authors concluded that groundwater colloids appear to be present in most subsurface environments and that the composition and concentration of colloids can be correlated with the type of site examined. For example, higher colloid concentrations were found at hydrogeologically disturbed areas, while lower concentrations were found at deep, geologically stable sites. They also concluded that the size of groundwater mobile colloids ranged from 10 to 1000 nm and their concentrations ranged from 0.1 and 100 mg/L. There is considerable debate on whether colloids sampled from natural systems are mobilized due to the sampling technique. The reader interested in this topic is referred to Backhus et al. (1993), Puls et al. (1992), and Puls (1990).

Perturbations in solution chemistry, aquifer hydraulics, and rainfall infiltration can generate colloids (Ryan and Elimelech 1996). At a site in the southwestern United States, changes in solution chemistry due to water infiltration through a coal-ash disposal site increased the number of silicate colloids, which was not observed in adjacent wells (Gschwend et al. 1990). The change in chemistry, which released the colloids from the matrix, could also enhance the matrix permeability. In contrast, iron-phosphate colloids were formed in situ at a Cape Cod site in Massachusetts (Gschwend and Reynolds 1987). These colloids formed as a precipitate of phosphate from the sewage plume and iron released from the matrix because of anoxic conditions. These and other studies (Seaman et al. 1995, Ryan and Gschwend 1994) have illustrated that colloids are generated at perturbed sites and that the absence of colloids in pristine environments does not preclude them as a mechanism at contaminated sites.

1.1.3 Non-Radioactive Contaminant Transport with Colloids

The presence of colloids in subsurface environments is only important if they sorb contaminants. The earliest studies on colloid-facilitated transport focused on the mobility of hydrophobic pesticides and herbicides. The presence of natural organic matter (NOM), such as humic and fulvic acids, increased the solubility and mobility of DDT, phenanthrene, naphthalene, and napropamide (Kan and Tomson 1990, McDowell-Boyer et al. 1986, Means and Wijayarante 1982, Ballard 1971). McCarthy and Jimenez (1985) found that there was a direct relationship between the chemical hydrophobicity and its affinity for humic acids. It is not clear if the hydrophobic contaminants are adsorbed to the NOM or if they are trapped in micelles or hemimicelles. In either case, the stability and transport observed were due to colloidal behavior.

Magaritz et al. (1990) examined the impact of 20 years of irrigation with secondary sewage effluent and agricultural spraying on metal distribution in the unsaturated (30 m) and saturated sediments of an aquifer in Israel. The authors found that zinc (Zn), copper (Cu), and silver (Ag) were associated with colloidal particles in concentrations two to ten times higher than fine sediments in both the saturated and unsaturated zones. However, it was not clear if the colloids were mobile or immobile in the aquifer. In contrast, the concentrations of iron (Fe) and manganese (Mn) were higher in the fine sediments. All the metals were present in the saturated zone, which indicates that in the past, chemical conditions of the aquifer permitted metal migration to the saturated zone. The method by which the samples were collected precludes conclusions about how the metals migrated. However, it does demonstrate that a thick unsaturated zone does not protect groundwater from contamination by heavy metals.

A study of landfill leachate by Gounaris et al. (1993) provided more substantial evidence for the association of metals with colloids. Zinc was found in the dissolved phases as well as associated with colloids from 1.3 nm to $10\text{ }\mu\text{m}$. In contrast, lead (Pb) was found only in the $1\text{-}10\text{ }\mu\text{m}$ fraction and chromium (Cr) was found in the humic fraction ($1.3\text{-}10\text{ nm}$). In this study by Gounaris et al. (1993), the metal concentration was not of environmental significance, but does demonstrate a relationship between stable colloidal fractions and metals. In addition, the authors examined the distribution of hydrophobic contaminants and found that they were strongly associated with colloids. Colloids ranging in size between 100 nm and $1\text{ }\mu\text{m}$ were stable and had a high sorptive capacity, which would facilitate transport. This study clearly demonstrates that both metals and hydrophobic contaminants can sorb to colloidal fractions. Unfortunately, the area around the landfill was not sampled to determine if the colloids were mobile.

1.1.4 Radioactive Contaminant Transport with Mobile Colloids

Because many radionuclides strongly adsorb to mineral surfaces, one of the key assumptions adopted in transport models is that the radionuclides, once adsorbed, are immobile. However, considerable laboratory and field evidence indicates that colloidal materials are mobile in groundwater, and it is possible that adsorbed radionuclides could be transported by these mobile colloids [reviewed by McCarthy and Zachara (1989) and McCarthy and Degueudre (1993)].

Several laboratory studies have been conducted to evaluate whether radionuclides associated with mobile colloids can move through sediments or fractured media. Colloid formation in the presence of waste forms also has been studied extensively (Kim et al. 1985, Bates et al. 1992, Buck et al. 1993, Feng et al. 1993). Spallation and nucleation have been proposed to be the mechanism of colloid genesis during the waste glass reaction (Bates et al. 1992, Feng et al. 1994). The colloids have been identified as inorganic colloids such as zeolites (Bates et al. 1992, Buck et al. 1993, Feng et al. 1993). Plutonium and Am released from waste forms have been shown to be predominantly in the colloidal as opposed to the dissolved form (Kim et al. 1985, Bates et al. 1992). The concentration of Pu and Am associated with the colloidal form were found to be orders of magnitude greater than their respective concentrations in the dissolved phase (Bates et al. 1992). The size of Pu and Am colloids

is normally <40 nm (Kim et al. 1985). Conversely, Np has been found to be released from waste forms predominantly in the dissolved form (Bates et al. 1992).

No studies have measured directly the extent to which radionuclide-bearing colloids move through unsaturated systems. A few field studies have been conducted to evaluate colloid facilitated transport (Buddemeier and Hunt 1988, Kaplan et al. 1994, Degueudre et al. 1989, Penrose et al. 1990). Buddemeier and Hunt (1988) reported that essentially 100% of the radioactive Ce and Eu in the Nevada Test Site were associated with colloids. Travis and Nuttal (1985) observed that Pu and Am migrated more than 30 m downward through unsaturated tuff material over the course of approximately 30 years. Laboratory experiments using the tuff material suggested that colloid forms of Pu and Am were responsible for the rapid migration. Investigations of four waste plumes in groundwater at the Chalk River Nuclear Laboratories in Canada were described by Champ et al. (1984). The authors suggested that organic ligands enhanced the mobility of Co, Ce, Cs, Eu, Sb, and Zr through the formation of mobile complexes. They reported detection of significant particulate nuclides on the 400-nm filter for ^{60}Co , ^{95}Zr , ^{106}Ru , and ^{137}Cs , and ^{140}Ce .

Based on laboratory experiments using site-specific materials, Pu and Am transport at Los Alamos National Laboratory was predicted to be limited to less than a few meters (Penrose et al. 1990). However, both radionuclides were detected in monitoring wells as far as 3390 m down-gradient. The Pu in the groundwater was found to be in a filterable fraction, whereas U, Am, and Cm were primarily in a nonfilterable fraction. The Pu was difficult to exchange, suggesting to the researchers that the Pu was likely precipitated onto the colloids.

1.1.5 Colloid Mobility under Saturated Conditions

The transport of colloids under saturated conditions has been investigated in the laboratory and in the field. Column studies on NOM transport have shown that they are highly mobile and that, depending on the experimental conditions, even the hydrophobic NOM can move through the columns (McCarthy et al. 1993, Dunnivant et al. 1992). Enfield et al. (1989) took the research a step further and demonstrated that not only do humic acids and other macromolecules move through saturated columns, but they also enhance the transport of pyrene and hexachlorobenzene.

Laboratory experiments indicate that colloids can be transported under saturated conditions. Natural systems are more complex, so it is also important to investigate colloid transport in the field. In a field experiment, Harvey et al. (1989) injected indigenous bacteria, latex microspheres, and a conservative tracer into an aquifer at Cape Cod. In the forced-gradient experiment, the bacteria broke through ahead of the conservative tracer and in higher concentration than the microspheres. The microspheres interacted with the aquifer, and their behavior could be predicted by filtration theory. This experiment shows that colloidal particles can indeed move in the field. However, the chemistry and the behavior of the bacteria were not fully characterized. Therefore, conclusions could not be drawn as to the mechanisms that affect transport, or predictions made as to the behavior of bacteria in other systems.

In another field study, Higgs et al. (1993) utilized laboratory experiments to predict what would happen under field conditions. Using two polymeric and two particulate colloids that ranged from 1 to 100 nm, the researchers found that the composition and packing of the columns affected the reproducibility of the data. For example, in columns where the aquifer material was not washed, the colloidal particles sorbed to mobile clay particles, which resulted in a range of colloid sizes and affected transport. The experiments were repeated on washed aquifer material and the colloid breakthrough allowed predictions to be made for the field experiments.

The field experiments were carried out in a well-characterized glacial aquifer confined by clay horizons. The colloids and tracers were released 0.94 m downgradient from the recharge well, and care was taken to ensure that they were uniformly mixed in the well before release. Two of the

colloids were not recovered in the field experiment as predicted. Silica and fulvic acid colloids were recovered, and based on the studies previously discussed, these colloids also are likely to bind with metals or radioactive contaminants. These experiments were well thought out and executed and provided the first link between laboratory and field-scale experiments for predictive modeling.

1.1.6 Colloid Mobility Under Unsaturated Conditions

Several authors have investigated the generation and transport of colloids in the unsaturated zone (Kaplan et al. 1996c, Kaplan et al. 1993, Amrhein et al. 1993, Powelson et al. 1990). Based on their results, it is still not clear what mechanisms control the transport of colloids in the subsurface, especially under semiarid conditions. Wood and Petraitis (1984) studied the partial pressure of carbon dioxide (CO₂) to understand the carbonate chemistry of water recharge to the Ogallala aquifer in Texas through a thick unsaturated zone. The study site was semiarid and had an average infiltration rate of 0.25 cm/yr. The authors found that the pressure of CO₂ was greater at 36 m below the surface than at the surface, which contradicted expected CO₂ distribution. They concluded that CO₂ was generated at depth by aerobic bacteria from particulate organic matter that was transported from the surface. This conclusion was consistent with isotopic analysis and the fractions of NOM in groundwater. This study provides strong evidence of NOM mobility in the unsaturated zone, but the mechanism by which it was transported is not understood.

At a site in Tennessee, the transport of dissolved organic carbon (DOC) through a forested hill slope was studied during rainfall events (Jardine et al. 1990). The majority of the DOC recovered during the storm events was from the surface horizons and traveled through preferential flow paths. The authors found that at the surface horizon, the concentration of DOC was highest in the large pores. As the depth increased, the highest concentrations of DOC were found in small pores. The rainfall intensity determined which pores contributed to the flow of DOC. The study investigated the flow through only the surface 3 m of soil, so it does not answer the question raised in the previous study of whether the transport of DOC at depths occurs only during recharge or if the DOC is mobile in water films between rainfall events.

In an attempt to understand how colloids are transported in the unsaturated zone, glass micromodels were used to visualize their mobility (Wan and Wilson 1994a, Goldenberg et al. 1989). Both studies showed that hydrophobic colloids preferentially sorbed to the air-water interface, and release of the particles was not observed. Wan and Wilson (1994a) found that the degree of attachment was dependent on the surface charge, hydrophobicity, and ionic strength. In the study by Goldenberg et al. (1989), the flow was varied to force the movement of air bubbles through the pore network. They found that bubbles could transport 20-50 times more hydrophobic colloids than the average suspension. It was also noted that the bubbles can be elongated, permitting them to pass through narrower pore throats. Neither study examined the effect of a continuous air phase on the transport of colloids. These studies were the first step in determining the mechanism for colloid transport through the subsurface. However, because the studies were small and two-dimensional, it is difficult to draw conclusions beyond the fact that the air-water interface plays a key role in unsaturated colloid transport. The micromodels did not provide insight into the effects of straining, entrapment into interstitial spaces, movement in small versus large pores, effects of volumetric water content, and changes in porosity that could potentially affect colloid mobility. In addition, these studies were conducted in the high range of saturation, which could not be determined due to the two-dimensional nature of the micromodel.

In a follow-up study, Wan and Wilson (1994b) examined colloid movement through unsaturated columns. They found that there was some variability in the breakthrough of hydrophilic and hydrophobic colloids as a function of air saturation. They attributed the reduction in mass recovery to colloid interaction with the air-water interface. Based on their micromodel studies, they estimated that 8% of the hydrophilic colloids were retained at the air-water interface. This is inconsistent with the observation by Williams and Berg (1992), who found that hydrophilic silica and carboxyl-

modified latex particles did not enter the air-water interface. In their column studies, they examined only one colloid size for the hydrophobic and hydrophilic colloids. These colloids were approximately 200 nm, compared to 1000 nm in their micromodel study. The smaller colloid size is more likely to be affected by Brownian diffusion than the 1000 nm colloids, which are more likely to be affected by hydrodynamic forces. Therefore, it is possible that the retention of 8% of the hydrophilic colloids was due to retention mechanisms other than the air-water interface.

Williams and Berg (1992) also concluded that, due to tortuosity, the transport of hydrophobic colloids along the air-water interface was not a viable mechanism for colloid transport in porous media when the air phase is continuous. However, they provided no evidence that the gas phase was distributed uniformly in the column. In addition, the water and gas saturation was an average value determined by column weight. It is highly probable that the water content increased from the top of the column to the bottom. Because it is difficult to conclude that the air phase was continuous through the entire column, the transport of hydrophobic colloids along a continuous air-water interface may still be a potential transport mechanism.

1.2 Objectives

The objectives of this study were to evaluate three aspects of colloid facilitated transport of radionuclides as they specifically relate to the LLW-PA. These objectives were:

1. Determine if the chemical conditions likely to exist in the near and far field of the proposed disposal site are likely to induce flocculation (settling of colloids from suspension) or dispersion of naturally occurring Hanford colloids
2. Using models based on filtration theory, identify the important mechanisms likely to be involved in the removal of colloids moving through a saturated Hanford sediment
3. Determine if colloids can move through unsaturated porous media.

1.3 Scope

This report describes three sets of experiments or calculations: effects of groundwater chemical composition on the dispersion/flocculation of colloids, colloid filtration by saturated porous media, and colloid transport through an unsaturated porous media. The first set of experiments, the effect of groundwater chemistry on the stability of colloid suspensions, used <1000-nm colloids collected from a Hanford sediment to determine the critical flocculation concentrations (CFC). This parameter identifies the minimum groundwater electrolyte concentration to induce colloid flocculation. If the groundwater has an electrolyte concentration greater than this critical value, than flocculation is expected to occur; if the groundwater has an electrolyte concentration less than this critical value, than dispersion is expected to occur. These critical values were measured for a series of environmental conditions (pH and sodium adsorption ratios) expected to exist in the near and far fields of the proposed LLW disposal site. Once the CFC were experimentally determined, expected near and far field chemical conditions were compared to these CFC, thereby providing an indication of the propensity of these systems to induce flocculation or dispersion of colloids.

The scope of the second study, colloid filtration by saturated porous media, was to conduct calculations to identify the important mechanisms responsible for colloid removal from saturated porous media. The model used in these calculations is based on filtration. A number of simulations relevant to the proposed LLW disposal site were conducted to evaluate the effect of varying the size of sediment particles, colloid particles, and flow rate on colloid transport.

The scope of the third study, colloid transport through an unsaturated porous media, was to generate experimental data to evaluate if colloids, once generated and in a stable suspension, could move through a column containing sand. Unsaturated conditions in the sand were created using an unsaturated flow apparatus (UFA). Polymer colloids with a density similar to that of water were used in these studies so no experimental artifact associated with the centrifugal force of the UFA would be created. The coarse sand used in the column experiments represented a simplified approximation of the sediment in the 200 East Area. Colloid size and degree of saturation were the dependent variables in these experiments.

2.0 Suspension Stability of Colloids Collected From Hanford Sediments as a Function of pH and Sodium Concentrations

2.1 Materials and Methods

Critical flocculation concentration tests were conducted to determine the minimum ionic strength needed to induce suspended colloids to induce flocculation of a clay suspension. As described in the introduction of this report, for colloids to be mobile through porous media they must not only exist in the ground, they must remain in suspension. Laboratory studies have demonstrated a three-way interaction of electrolyte concentration, dissolved sodium concentration, and pH on clay dispersion (van Olphen 1977). This interaction is predicted by electrical double-layer theory, in which repulsive forces between expanding double layers increase as electrolyte concentration decreases and dissolved sodium and pH increase (van Olphen 1977). Critical flocculation concentration tests involve placing a clay suspension in a series of tubes containing a wide range of electrolyte concentrations. The suspensions are then permitted to settle. At electrolyte concentrations greater than the CFC the colloids flocculate. At electrolyte concentrations less than the CFC the colloids remain in suspension. The CFC metric is empirical and is operationally defined (van Olphen 1977).

Trench AE-3 sediment from the Hanford Site was used in this study. The chemistry, mineralogy and particle size distribution of this soil was previously described by Kaplan et al. (1996b). Briefly, it is a silt loam collected from the side of the AE-3 trench in the 200 West Area on the Hanford Site. It has a pH of 8.3, surface area of 14.8 m²/g, and gravel, sand, silt, and clay percentages of <1, 41, 50, and 9%, respectively. The clay fraction (<2000 nm) is primarily composed of smectite (57%), illite (19%), and vermiculite (14%).

Colloids used from the critical flocculation tests were collected from a 50-g/L sediment suspension using a method modified from Gee and Bauder (1986). The suspensions were shaken overnight and then permitted to settle for 28 hr and 10 min, at which time the top 9.0 cm of the suspensions were recovered. This depth and time were calculated using Stoke's Law to remove particles with a hydrated radius of 1000 nm. The 1000-nm size has been cited as the largest colloid that can pass through aquifer matrix materials (McCarthy and Degueldre 1993, Kaplan et al. 1993, Kaplan et al. 1995, Kaplan et al. 1996c). The <1000-nm fraction collected from the sediment was diluted to 0.7 mg/L with distilled water; this was used as the stock for the CFC tests. Four aliquots of the stock colloid solution were adjusted to pH 7.0, 8.3 (no adjustment), 9.3 and 10.3 with either 1 M NaOH or 1 M HCl. Using NaCl and CaCl₂, four solutions of varying sodium adsorption ratios (SAR) were used in this study: infinity, 60, 5, and 0 (mmol_c/L)^{0.5}. Sodium adsorption ratios are defined as

$$\text{SAR} = \frac{[\text{Na}^+]}{(0.5 [\text{Ca}^{2+} + \text{Mg}^{2+}])^{0.5}} \quad (2.1)$$

where the square brackets refer to concentrations in mmol_c/L. Sodium adsorption ratios therefore has units of (mmol_c/L)^{0.5}, but for convenience, units are commonly omitted.

Following the CFC procedure of van Olphen (1977) and modified by Miller et al. (1990), 3 mL of the 0.7-g/L clay suspension were placed in a series of 5-mL cuvettes. One mL of the treatment solutions was placed in each cuvette. The duplicated treatments were shaken by hand for approximately 10 sec and then permitted to settle for 3 hr. The concentration of clay remaining

in suspension was estimated by measuring optical density at 420 nm, which is the optimal wavelength for adsorption by clays. The electrolyte concentration that induced a 95% removal (flocculation) of the clay was defined as the CFC. Freshly prepared <1000-nm clay fractions were used in these tests. The clay suspension closest to the CFC were centrifuged, and the supernatant was analyzed for pH and electrical conductivity. Electrical conductivity has been empirically related to electrolyte concentration.

2.2 Results and Discussion

The results from the critical flocculation concentration (CFC) experiment are presented in Figure 2.1. Four pH and four SAR levels were evaluated in duplicate at 16 electrolyte concentrations. This represents the results from 512 separate tests (512 cuvettes = [2 reps] x [4 pH] x [4 SAR] x [16 electrolyte concentrations]).

An increase in the CFC indicates that the colloids are more dispersive and therefore require higher concentrations of electrolyte to induce flocculation. As expected, there was a propensity for the CFC to increase as the pH and the Na:Ca molar ratio increased (Figure 2.1). The effect of pH was less than the effect of the SAR on the CFC (Figure 2.1).

As a first approximation, one can evaluate whether uncontaminated Hanford groundwater would induce flocculation or dispersion of these <1000-nm colloids by comparing the SAR, pH, and total electrolyte concentration of the groundwater to the CFC values presented in Figure 2.1. For the Hanford groundwater, the pH was 8.1, electrolyte concentration 9.86 mmol/L, and the SAR was 1.04 (mmol/L)^{0.5} (Table 2.1). This pH and electrolyte coordinate is identified in Figure 2.2. A comparison to the pH- electrolyte concentration coordinate to the CFC values for SAR 5 (mmol/L)^{0.5} would be a conservative estimate of the likelihood that the groundwater would cause dispersion. Since the groundwater pH-electrolyte concentration coordinate is above the CFC for SAR = 5, flocculation of the colloids is expected. This indicates that, under these experimental conditions, the natural electrolyte concentration of Hanford groundwaters is above the CFC for this system, and colloids introduced into this system would flocculate.

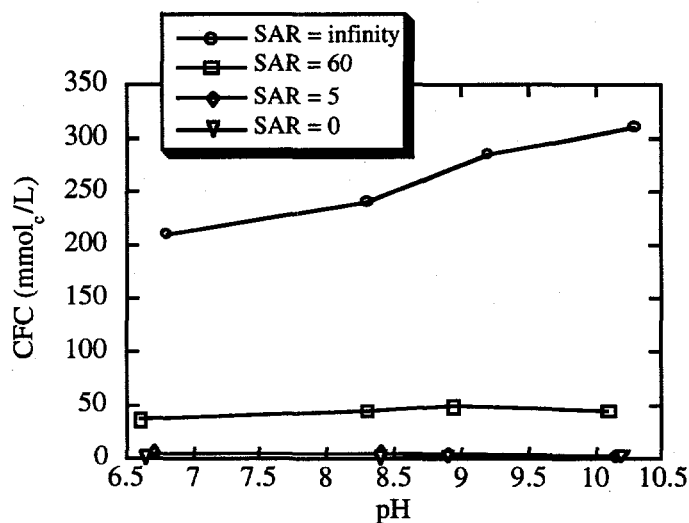


Figure 2.1. Critical Flocculation Concentrations (CFC) of Suspension of the <1000-nm Fraction of a Hanford Sediment (Trench AE-3) as a Function of pH and Na:Ca Molar Ratios. The CFC is the Minimum Electrolyte Concentration to Induce Flocculation of Suspended Colloids.

Table 2.1. Chemical Composition of an Uncontaminated Hanford Groundwater (Well: 6S3-25 from 1985 to 1990) and Estimated Plume Concentrations in the Near Field

	Far Field		Near Field ^(a)	
	mmol/L	mmol/L	mmol/L	mmol/L
Ca ²⁺	1.22	2.44	7.8 x 10 ⁻⁴	1.56 x 10 ⁻³
K ⁺	0.25	0.25		
Mg ²⁺	0.60	1.20		
Na ⁺	1.40	1.40	545	545
Cl ⁻	0.76	0.76		
SO ₄ ²⁻	0.78	1.56		
HCO ₃ ⁻	2.25	2.25		
Total Cations	3.47	5.29		
Total Anions	3.79	4.57		
Total Electrolyte	7.26	9.86	545	1090
pH	8.1 ^(b)			
SAR		1.04 ^(b)		

(a) Near field groundwater concentrations generated from AREST code. Results from Mann et al. 1996. The data selected from AREST simulations include the highest Na and pH levels reported by this simulation (which occurred in the year 19,970, line 1325 of the simulation).

(b) pH is unitless; SAR has units of (mmol/L)^{0.5}

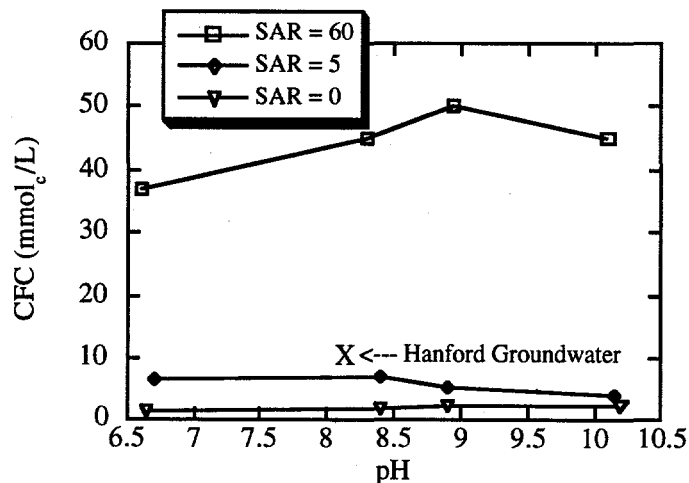


Figure 2.2. Experimentally Derived Critical Flocculation Concentrations (CFC) of Hanford Sediment Colloids (<1000 nm) as a Function of Sodium Adsorption Ratio and pH. The pH- Electrolyte Concentration Coordinates of an Uncontaminated Hanford Groundwater is Identified with an "X." The Fact that the pH-Electrolyte Coordinates of the Natural Groundwater Exist Above the CFC Line Indicates that Colloid Flocculation is Expected.

The other extreme of environmental conditions likely to exist in the LLW-PA disposal area is in the near field. In the near field, sodium concentrations and pH are expected to be much higher and calcium concentrations much lower than in the far field. These are precisely the chemical conditions likely to keep colloids in suspension. Following a similar logic as used above for the far-field data, the pH- electrolyte concentration coordinates for the far field have been superimposed over the CFC data (Figure 2.3). The pH (pH 10), sodium (545 mmol_e/L), and calcium 1.56×10^{-3} mmol_e/L concentrations used in these calculations (Table 2.1) were taken from a simulation conducted with the AREST code (Chen et al. 1997, Mann et al. 1996). These data represent the most dispersive conditions, the highest sodium concentrations, and highest pH levels calculated for the near field. The SAR of the near field plume was 19,514 (mmol_e/L)^{0.5}, which can be approximated by the SAR = infinity data presented in Figure 2.3. As was the case with the far-field groundwater, the pH-electrolyte concentration coordinate is well above the CFC-infinity line. This indicates that if suspended colloids were to enter into water of this chemical composition, they would likely flocculate.

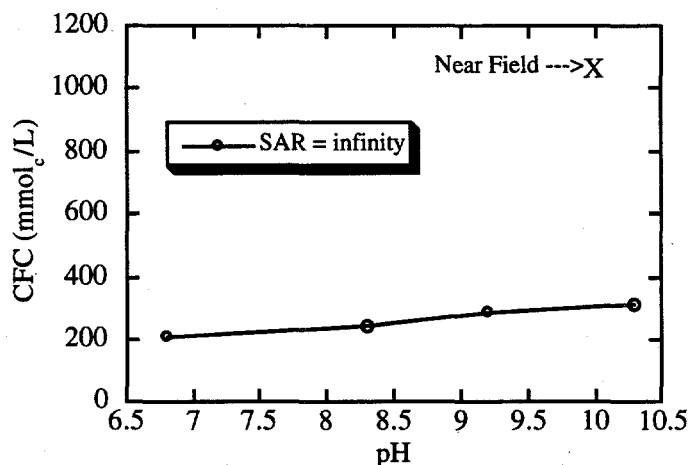


Figure 2.3. Experimentally Derived Critical Flocculation Concentrations Coefficients (CFC) of Hanford Sediment Colloids (<1000 nm) in Sodium solutions (SAR = infinity) as a Function of pH. The pH- Electrolyte Concentration Coordinate of a Theoretical Near Field Groundwater is Identified With an "X." The Fact that the pH-Electrolyte Coordinates of This Theoretical Near Field Water Exist Above the CFC Line Indicates that Colloid Flocculation is Expected.

3.0 Colloid Transport Through Saturated Systems

3.1 Theory

A semi-empirical model based on filtration theory was used to model colloid retention by a porous media. The model was originally used by civil engineers for describing particle removal by porous beds in sewage waste treatment plants. Some success has been obtained in applying this model to uncharged, homogeneous particle systems (Spielman and Goren 1970, Yao et al. 1971, Elimelech and O'Melia 1990). The limited applicability of filtration theory to describe particle transport through porous media has been discussed by McDowell-Boyer et al. (1986). They concluded that data were needed on particle retention, aggregate formation, permeability reduction, and the potential for erosion by changes in flow or solution chemistry before colloid transport through a natural aquifer could be predicted. Given these limitations, we intend to use the results from these calculations as a first approximation of the removal processes that may act on colloids in the proposed Hanford LLW disposal site. Thus, these calculations will be used in a qualitative, not quantitative, manner.

Several studies have provided an in-depth review of this model (Yao et al. 1971, McDowell-Boyer et al. 1986, Tien 1989); only a brief description follows. Suspended particles moving through a porous system can be removed from the mobile phase by four processes: diffusion, interception, sedimentation, and electrostatic attraction. Particle removal is characterized by the single-collector efficiency parameter (η),

$$\eta = \frac{\text{rate at which colloids strike the media particles}}{\text{rate at which colloids flow toward the media particles}} \quad (3.1)$$

where the media particles are in the immobile solid phase. The term "collector" emphasizes the wastewater treatment origin of the model.

A suspended particle is subject to random bombardment by molecules in the suspending medium, resulting in Brownian movement of the particle. The term diffusion is used to describe mass transport by this process. Particle capture by diffusion followed by adsorption is generally limited to particles less than 1000 nm in diameter (Herzig et al. 1970, Yao et al. 1971). The single-collector efficiency due to diffusion (η_D) is defined by

$$\eta_D = 0.9 \left(\frac{kT}{\mu d_c d_m v_0} \right)^{\frac{2}{3}}, \quad (3.2)$$

where k is Boltzmann's constant, T is absolute temperature, μ is viscosity, v_0 is the water velocity, d_m is the media particle (sand) diameter, and d_c is the suspended particle diameter.

Interception describes the process by which suspended particles are removed from the mobile phase because of their size. The role of interception increases as the ratio of media-particle diameter to suspended-particle diameter increases. Suspended particle capture resulting from collisions with media particles is one form of interception. Sieving is another form of interception. Single-collector efficiency resulting from interception (η_I) is defined by

$$\eta_I = \frac{3}{2} \left(\frac{d_c}{d_m} \right)^2 \quad (3.3)$$

Interception is independent of influent particle concentration and flow rate.

The path of the particle is influenced by the combined effects of the buoyant weight of the particle and fluid drag on the particle. This transport process is called gravitational sedimentation. The single-collector efficiency due to gravitational sedimentation (η_G) is defined by

$$\eta_G = \frac{(\rho_{sp} - \rho_w)gd_c^2}{18v_0\mu} \quad (3.4)$$

where g is gravitational acceleration, and ρ_{sp} and ρ_w are the densities of the suspended particle and water, respectively. Equation 3.4 indicates that increases in water velocity will decrease η_G .

The single-collector efficiency resulting from electrostatics was assumed to be negligible. It was assumed that if the colloids were generated from detrital material from the negatively charged aquifer, the colloids would also have a negative charge; thereby creating repulsive, not attractive, forces.

The single-collector efficiency values were converted into clean-bed filter coefficients. These latter terms have more intuitive meaning and furthermore and are easily measured (Kaplan et al. 1996a). The clean-bed filter coefficient, λ_0 , is an index of the propensity of a clean sediment (a sediment without captured Fe^0 particles) to remove suspended particles from the mobile phase. The λ_0 in units of reciprocal distance is defined as

$$\lambda_0 = \frac{-\log\left(\frac{C}{C_0}\right)}{L} \quad (3.5)$$

where L is the column length (cm), C is the effluent particle concentration at the time of the tracer breakthrough ($g L^{-1}$), and C_0 is the influent particle concentration ($g L^{-1}$) (Herzig et al. 1970). The λ_0 term has been found to be a reasonable parameter for describing systems of fast moving colloids (>1 $cm min^{-1}$) and influent colloid concentrations of <1 $g L^{-1}$ (Herzig et al. 1970). Implicit in Equation 3.5 are a number of assumptions including: 1) λ_0 remains uniform during a filtration experiment, 2) λ_0 is uniform across the entire length of the column, 3) the kinetics of particle deposition follows a pseudo-first-order reaction with respect to suspended particle concentration, and 4) λ_0 is independent of influent particle concentration (Tien 1989).

The single-collector efficiency values were converted into clean-bed filter coefficients by using the following equation (Tien 1989):

$$\lambda_0 = \frac{3}{2}(1-\epsilon) \frac{\eta_{exp} U_{\infty}}{d_c v_0} \quad (3.6)$$

where U_{∞} is the approach velocity, η_{exp} is the experimentally derived collector efficiency, and ϵ is porosity. It was assumed that U_{∞} equaled v_0 because of the large and relatively uniform pore sizes in the sand columns.

3.2 Results and Discussions

The default values used in the filtration calculation are presented in Table 3.1. These values were selected to simulate conditions in the 200 East Area of the Hanford Site. The default flow rate value used in these calculation came from *Hanford Site Groundwater Monitoring for Fiscal Year 1996* (Hartman and Dresel 1997), which reported flow rates of 0.15 to 0.7 m/d (1.7×10^{-6} to 8.1×10^{-6} m/s). The colloid diameter size and density came from the "typical" values reported by McCarthy and Degueudre (1993), who did an exhaustive literature review of mobile colloid properties.

The effect of varying the groundwater flow rate on single-collector efficiency is reported in Figure 3.1. As the single-collector efficiency is increased, greater removal of colloids is expected to occur. Flow rates in the Hanford Site have been reported to vary from about 10 to 0.01 m/d (1×10^{-4} to 1×10^{-7} m/s) (Hartman and Dresel 1997). Flow rates in the 200 East Area have been reported to vary from 0.15 to 0.7 m/d (Hartman and Dresel 1997). Removal of mobile colloids in this system will be due primarily to gravitational settling and diffusion. Interestingly, the usual explanation for why colloids are removed from suspension, interception, is not important. In fact, interception would not likely become a dominant removal mechanism until the flow rate exceeded 10^{-2} m/s, which is a much faster flow rate than has ever been measured at the Hanford Site.

Table 3.1. Default Values Used in Calculations of Colloid Filtration by Porous Media in a Saturated System

Parameter	Value	Units
Boltzman constant	1.38×10^{-23}	kg m ² /s ² K
Temperature	285	K
Viscosity	1.003	kg/m s
Diameter of media particle (sediment particle)	1×10^{-3}	m
Diameter of mobile colloid	3×10^{-7}	m
Water velocity	3.26×10^{-6}	m/s
Mobile colloid density	2780	kg/m ³
Water density	997.8	kg/m ³
Gravitational acceleration	9.8	m/s ²

Figure 3.2 shows the results of the calculations that evaluate the effect of varying the average media particles (sediment) size that the mobile colloids pass through. As expected, as the sediment diameter decreases, the total single-collector efficiency (the sum of the individual removal mechanisms) increases. Only in clay-sized media would interception be the dominant removal mechanism. In sand- or gravel-sized media, gravitational settling and diffusion are the dominant mechanisms responsible for colloid removal.

In Figure 3.3, the effect that the mobile colloid diameter has on single-collector efficiency is evaluated. Again, either diffusion or gravitational settling are the dominant removal mechanisms, and interception plays a comparatively much smaller role. What is particularly interesting about these calculations is that there is a minimum of single-collector efficiency at about 300-nm mobile colloid diameter. This indicates that colloids smaller than 300 nm will tend to be removed by diffusion, whereas mobile colloids larger than 300 nm will be removed by gravitational settling. Furthermore, the minimum identifies the size colloid most likely to be transported through a system. The diameters of mobile colloids collected from field studies are always less than 1000 nm, and

frequently between 100 and 500 nm (McCarthy and Degueudre 1993), providing credence to the results presented in Figure 3.3.

Because it is a unitless parameter, the single-collector efficiency value is difficult to use in other equations. So this parameter was converted to a parameter that is more intuitive, the removal efficiency factor, by using Equations 3.5 and 3.6 (Figure 3.4). Figure 3.4 shows that a total single-collector efficiency of 10^{-3} is equivalent to a removal efficiency of about 10^{-2} cm^{-1} , or 97.7 % of the colloids entering a sediment (C_0) would remain in the mobile phase after the colloid plume moved 1 cm through the sediment (see Equation 3.5, the antilog of -0.01 is 0.977).

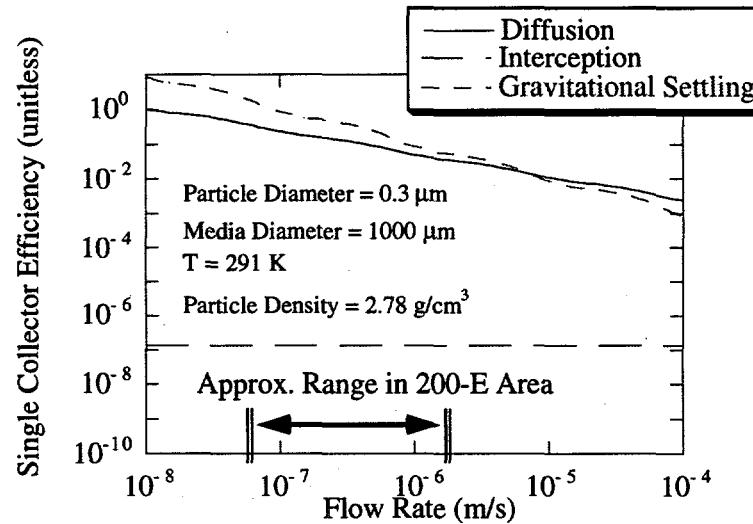


Figure 3.1. Effect of Groundwater Flow Rate on Single-Collector Efficiency (Equations 3.2, 3.3, and 3.4)

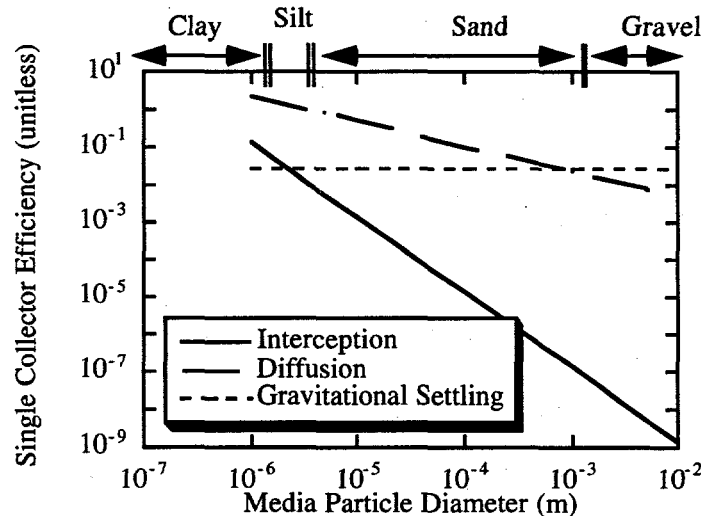


Figure 3.2. Effect of Media Particle (Sediment) Diameter on Single-Collector Efficiency (Equations 3.2, 3.3, and 3.4)

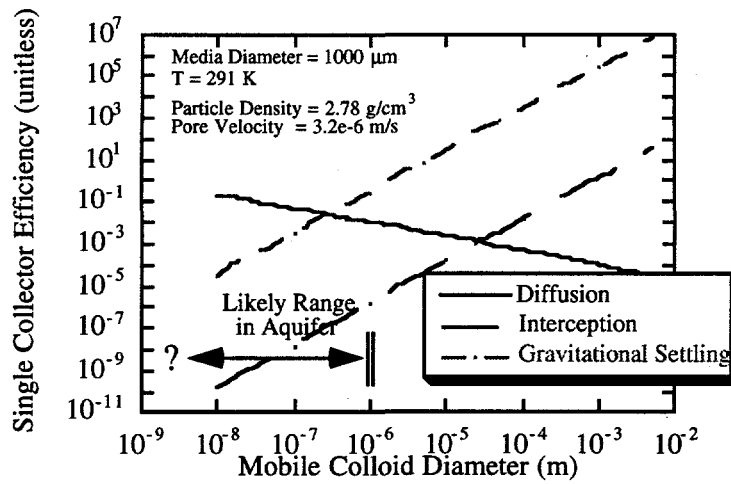


Figure 3.3. Effect of Mobile Colloid Diameter on Single-Collector Efficiency (Equations 3.2, 3.3, and 3.4)

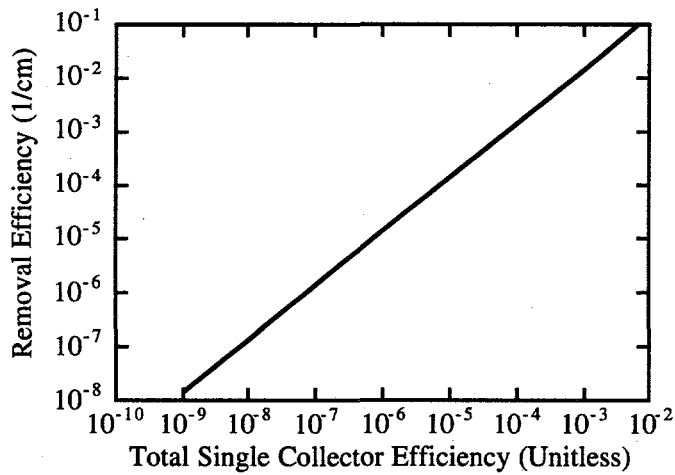


Figure 3.4. Relationship Between Total Single-Collector Efficiency and Removal Efficiency Factor (Equations 3.5 and 3.6)

4.0 Effect of Colloid Size and Degree of Saturation on Colloid Transport

4.1 Materials

4.1.1 Sand Characterization

A Unimin sand composed of 90% quartz; 9% Na-, K-, and Ca-feldspar; and 1% mica, based on particle counts under a microscope, was used for the column experiments (Figures 4.1, 4.2, and 4.3). The sand was wet-sieved. The fraction that passed through a 20-mesh sieve (850 μm) but was retained by a 40-mesh sieve (425 μm), was used for the experiments. This procedure resulted in a sand with a mean grain size of 650 μm . Finally, the sand was washed in Milli-Q water and allowed to air dry. Carbon analysis showed that the organic and inorganic fractions were both less than the detection limit. Inductively coupled argon plasma (ICP) analysis showed that the concentrations of Mg, Al, Fe, Ca, Na, K, and Mn, dissolved off the sand surface by 5% nitric acid, were present at or below the detection limit of the instrument (Thermo Jarrell Ash Atomscan 25). Therefore, no further treatment of the sand was necessary.

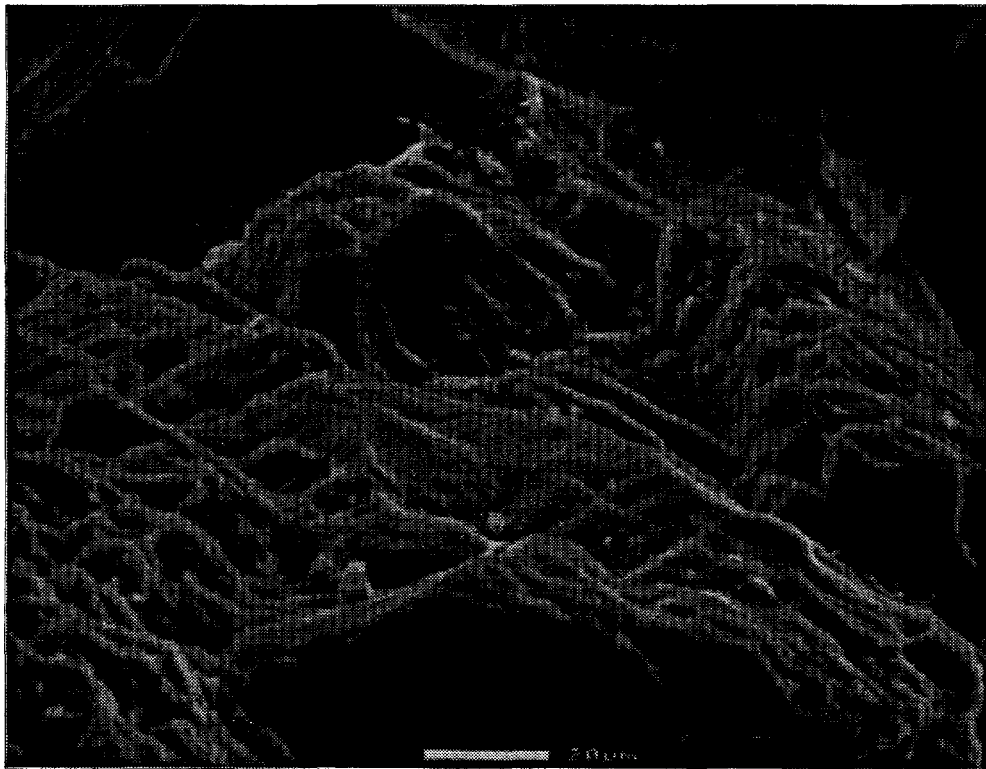


Figure 4.1. SEM Image of Quartz

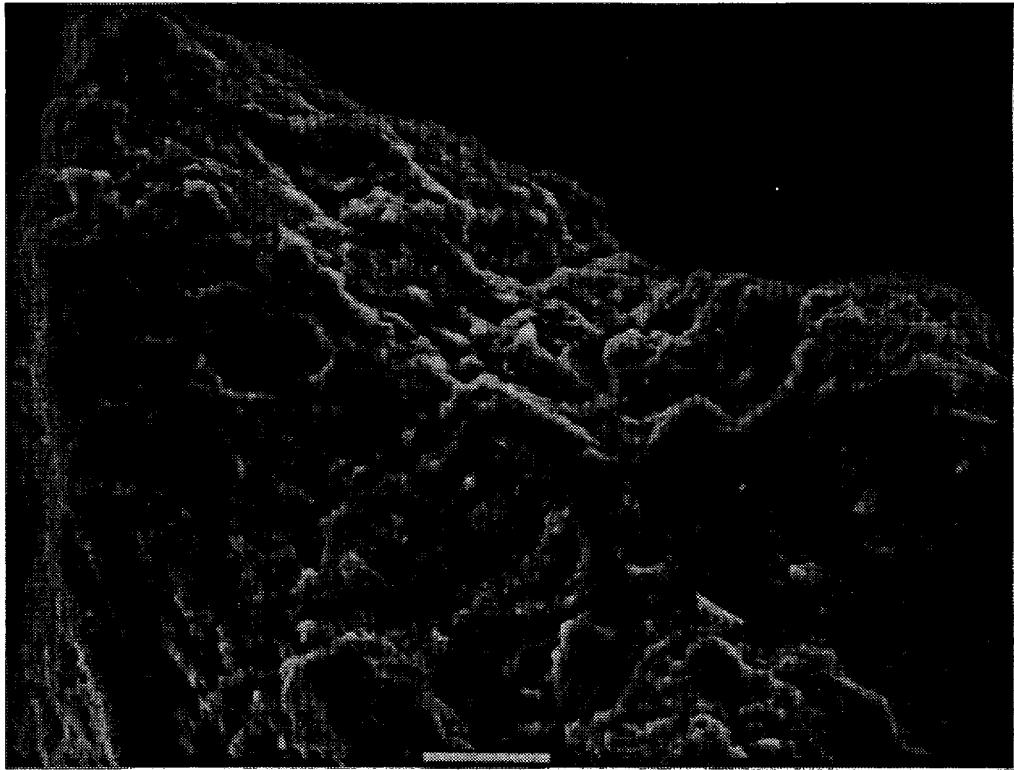


Figure 4.2. SEM Image of Feldspar

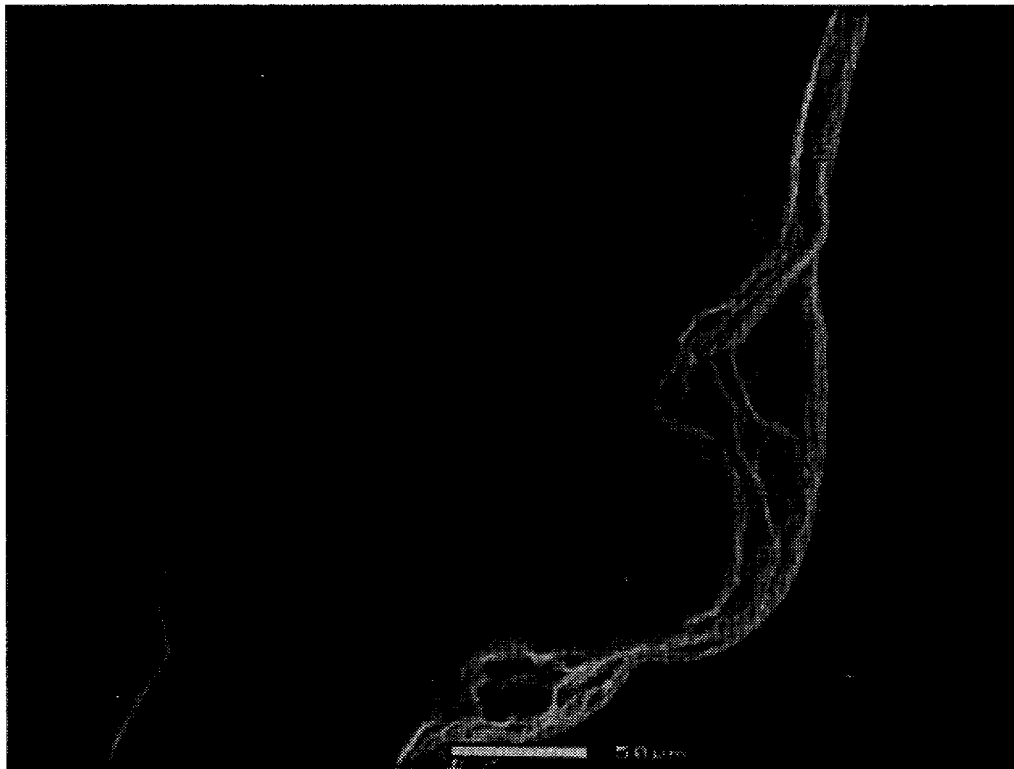


Figure 4.3. SEM Image of Mica

4.1.2 Colloid Quantification

Fluorescent latex microspheres were used as "idealized" colloids for the experiments. The polymer base of the colloids was polystyrene, which has a density of 1.05 g/cm^3 . The colloid stock suspensions were received from the manufacturer in distilled water and were stored between 2 and 10°C to prevent microbial growth. Polystyrene colloids, which did not contain surface functional groups, were purchased from Bangs Laboratories in Carmel, IN. These colloids were manufactured in the presence of surfactants such as sodium dodecyl sulfate or lauric acid.

Colloid suspensions were prepared on a weight basis by diluting the stock suspension to the desired concentration in water. The water used in all the experiments was distilled water further purified by a Milli-Q system (Millipore Corporation). Before dilution, the stock suspension was gently sonicated to disperse the colloids evenly. The low ionic strength of the Milli-Q water kept the colloids in suspension. All the suspensions were prepared and stored at 4°C in glass containers to prevent interference from those plasticizers (for example, phthalate) having fluorescent properties.

The initial colloid concentration for the experiments was approximately 2.5 mg/L , which is within the concentration range of $0.1\text{-}100 \text{ mg/L}$ reported for colloids at field sites (McCarthy and Degueldre 1993).

The colloids were analyzed on a Perkin-Elmer Luminescent Spectrometer L50. The excitation and emission values provided by the colloid manufacturer varied slightly from those observed. To determine the excitation wavelength, a 5-mg/L colloid suspension was scanned with the emission wavelength set to the value reported by the manufacturer. The wavelength at which the fluorescent intensity, which is an arbitrary unit, reached a maximum was used for the excitation wavelength (Ex_{max}). Next, three emission scans were done with the excitation wavelength set to Ex_{max} and $Ex_{\text{max}} \pm 5 \text{ nm}$. The fluorescent intensities of the three scans were then compared. If the fluorescent intensities from the $Ex_{\text{max}} \pm 5 \text{ nm}$ scans were greater than the fluorescent intensities from the Ex_{max} scan, then the excitation wavelength was systematically varied to determine the optimum wavelength.

The next step in the calibration was to adjust the slit widths for the excitation and emission wavelengths. The slit width determines the wavelength range over which light will be emitted or measured. The initial slit width was $\pm 5 \text{ nm}$ for both the excitation and emission wavelengths. Adjusting the slit widths can help dampen noise in the spectra and increase fluorescent intensity. The slit widths were systematically varied for a series of emission scans with the excitation wavelength fixed. Slit widths selected for the experiments were those where the fluorescent intensity was maximized without introducing noise into the spectra.

To determine the emission wavelength, colloid suspensions at five to six different concentrations, plus a water blank, were scanned with the excitation wavelength fixed. Typical emission scans can be seen in Figure 4.4, which shows the emission spectra for the 189-nm colloids. The emission scans for the other particles are given in Appendix A. The maximum emission value for each curve varied slightly as a function of the colloid concentration. The emission value that best represented the colloid concentration between 0.5 and 2.5 mg/L was selected as the emission value for the experiments. If the same particles are used in experiments at higher concentrations, a different emission value may be more appropriate. The excitation and emission wavelengths determined by this calibration technique are summarized in Table 4.1. These instrument settings were used for all subsequent experiments.

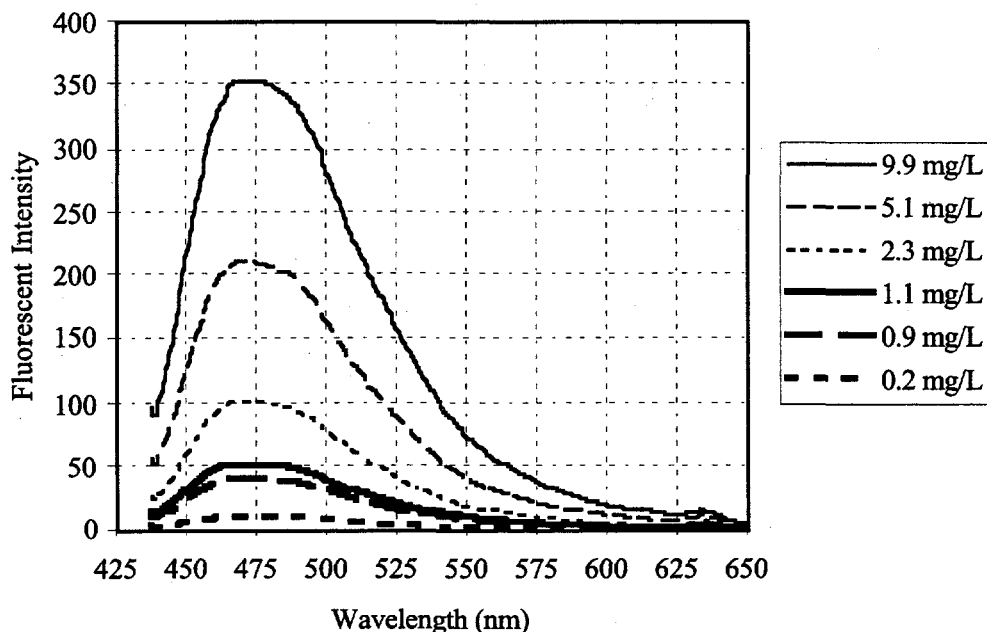


Figure 4.4. Emission Spectra of the 189-nm Colloids at Different Concentrations

Linear regression analyses were conducted for each colloid to ensure that the fluorescent intensity was linear over the range of the experiment. The colloid concentration was the independent variable, and the fluorescent intensity was the dependent variable. The fluorescent intensity of the water blanks was included in the regression. Emission spectra that significantly reduced the linearity of the calibration curve were not used in the analysis. Figure 4.5 presents the data points and the regression lines for the 189-nm colloids. The equation for the line and the degree of correlation (R^2) is listed on the figure. The calibration curves were linear over the entire range evaluated. Repeated measurement of colloid suspensions indicates that the analytical precision was ± 2 fluorescent intensity units. The calibration curves for the other colloids are given in Appendix A.

Table 4.1. Fluorescent Properties of Colloids

Colloid Properties			Excitation		Emission	
Size (nm)	Surface Groups	Fluorescent Dye	Wavelength (nm)	Slit Width (nm)	Wavelength (nm)	Slit Width (nm)
52	none	Yellow G	440	5	489	10
189	none	Coumarin 153	423	5	470	5
545	none	Yellow G	440	5	485	5
910	none	Acridine Orange	490	5	518	15
1900	none	DCM Orange	468	5	536	10

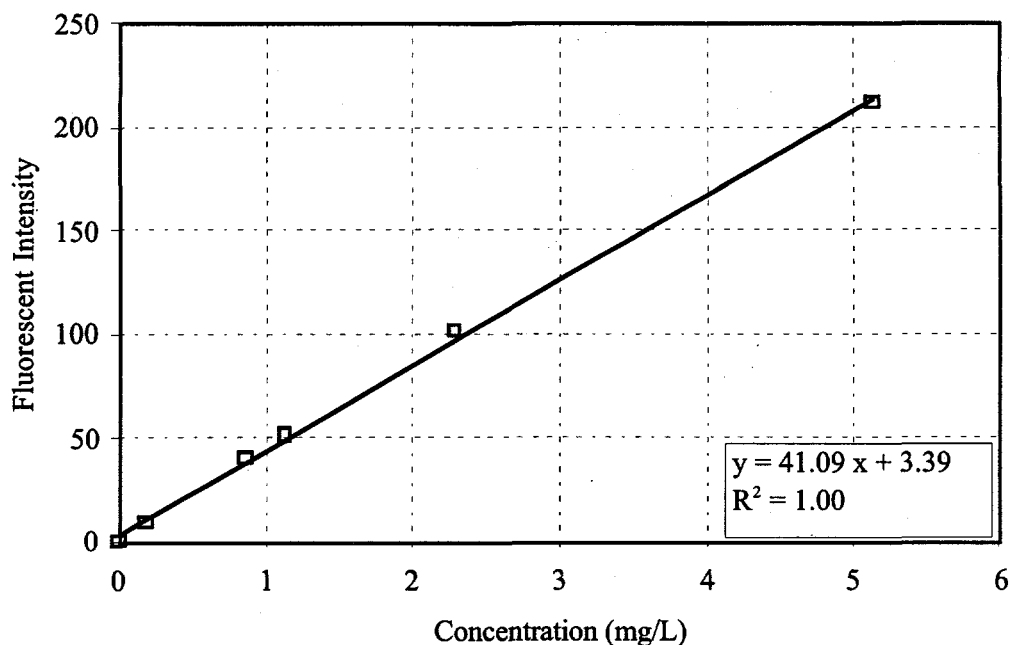


Figure 4.5. Calibration Curve for the 189-nm Colloids (Ex = 423 nm, Em = 470 nm)

4.1.3 Colloid Hydrophobicity Measurements

Contact angle measurements were made with a modified version of the technique used by Wan and Wilson (1994a). Contact angles measure the degree to which a liquid wets a solid surface. If the contact angle is $>90^\circ$, the surface is nonwetting. In contrast, if there is no contact angle, the liquid is considered wetting. For these measurements, a pellet or solid surface of the colloids was not available. Therefore, stock colloid suspensions were dried on glass microscope slides in a desiccator at room temperature to create a surface for contact angle measurements. The contact angle between the colloids and a drop of water will increase with the degree of hydrophobicity.

The hydrophobicity of these colloidal latex particles was assessed by determining the contact angle on a thick layer of dry particles that had been dried on a glass slide. For this purpose, a drop of triple distilled water was placed on the dried colloids with a pipet, and the final contact angle was measured with a Rame-Hart goniometer. The average of five to ten such measurements are shown in Table 4.2. For the hydrophilic colloids, the water was quickly imbibed into the solid mat and dispersed the colloids. The contact angle for these colloids was considered $<10^\circ$. The contact angles for the hydrophobic colloids were $<90^\circ$, due to the presence of some hydrophilic surfaces and the porous nature of the dried colloids. Contact angle measurements by this method must be considered as relative values.

The contact angles for the polystyrene without surface functional groups were generally large and indicate that the colloids were hydrophobic. The exceptions were the 52-nm and 910-nm colloids that had contact angles $<10^\circ$ and would be considered hydrophilic based on the contact angle measurement (Table 4.2). At this point, it is difficult to determine if the discrepancies are real or artifacts of the technique used. The incongruity that arose in the data will be discussed with the results.

Table 4.2. Relative Colloid Contact Angles (average of 5-10 replicates)

Latex with no surface functional groups	
Size (nm)	Contact Angle
52	<10°
189	74°
545	85°
910	<10°
1900	21°

Under unsaturated conditions, the degree to which colloids attach to the air-water interface depends on the degree of hydrophobicity or contact angle. Figure 4.6 schematically shows how the contact angle, ϕ , effects the degree of colloid immersion at the air-water interface. As the contact angle increases, the colloid becomes more hydrophobic, and the portion of the colloid immersed in water decreases. In contrast, hydrophilic colloids are always surrounded by a layer of water even at low volumetric water contents when the water film is less than the colloid diameter.

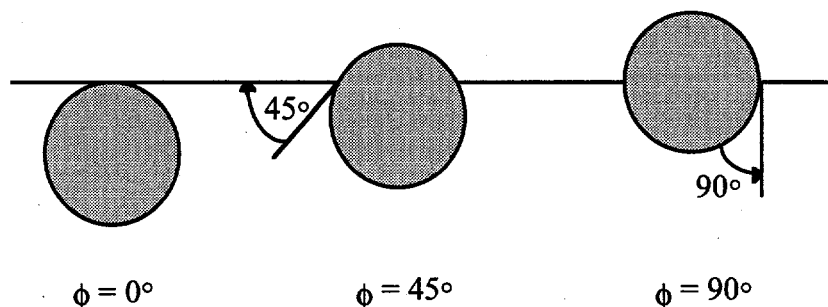


Figure 4.6. Effect of Contact Angle on the Degree of Particle Immersion at the Air-Water Interface

4.1.4 Colloid Zeta Potentials

Zeta potentials were measured with a Zeta Sizer 3 (Malvern Instruments) fitted with an AZ4 electrophoresis cell and on a Zeta Plus (Brookhaven Instruments Corporation) at $22 \pm 1^\circ\text{C}$. The two instruments were used to cover the range of colloid sizes. The Zeta Sizer 3 worked best for particles ≤ 500 nm, and the Zeta Plus worked best for particles ≥ 100 nm. The instrument calibration was verified with the AZ55 electrophoretic mobility standard (Malvern Instruments), which has a zeta potential of -55 ± 5 mV at 25°C . The standard was run at the beginning, middle, and end of the experiments to ensure measurement accuracy.

The colloid suspensions were prepared in a pH 7 buffer supplied by Malvern Instruments. The averages of two separate zeta potential measurements are shown in Table 4.3. The zeta potentials for all the colloids were similar and did not vary more than the machine accuracy of ± 5 mV. The exception was the 1900-nm colloids, which had a significantly lower zeta potential. The zeta potentials measured on both instruments corresponded well.

Table 4.3. Average of Two Zeta Potential Measurements for Latex Colloids and AZ55 Standards (-55 ± 5 mV)

Size (nm)	Surface group	ζ (mv) Malvern	ζ (mv) Brookhaven
Standard	Initial	-56	-51
Standard	Middle	-56	-53
Standard	Final	measurement error	-52
52	none	-44	-44
189	none	-48	-48
545	none	-45	-44
910	none	(a)	-49
1900	none	(a)	-10
(a) Outside optimum range of instrument.			

4.2 UFA/Colloid Transport

4.2.1 Saturated Column Experiments

Glass chromatography columns (5 cm (ID) x 10 cm (L)) with polypropylene ends were used for the experiments. The column diameter was selected to be at least 50x larger than the mean grain size to minimize the influence of flow along the column walls (Relyea 1980). The columns were dry packed with sand using a column vibrator. The weight of the column was taken before and after packing to determine the column porosity, n , using Equation 4.1,

$$n = 1 - \frac{\left(\frac{\text{weight of the sand (g)}}{\rho_{\text{sand}} \text{ (g/cm}^3\text{)}} \right)}{\text{column volume (cm}^3\text{)}}, \quad (4.1)$$

where ρ_{sand} is the density of the sand.

To maintain low flow rates and prevent contamination, a medical AVI Micro 210A Infusion pump manufactured by 3M was used for all the colloid experiments. The pump does not contain any valves that could trap the colloids. Instead, it uses a dual piston and rolling diaphragm mechanism to control flow within ± 2% through a disposable bladder, so the fluid never contacts the pump mechanism. The pump maintains a positive delivery pressure with a threshold of 9 psi (467 mm Hg).

The flow rate for the experiments was 20 ml/hr, which corresponds to a specific discharge, v , of 2.83×10^{-4} cm/s. The Reynolds number, Re , for flow-through porous media is defined as

$$R_e = \frac{\rho v d_m}{\mu}, \quad (4.2)$$

where ρ is the density of the fluid, d_m is the mean grain size, and μ is the viscosity (Freeze and Cherry 1979). Reynolds numbers between 1 and 10 are considered laminar, and the value for the saturated experiments was $R_e = 0.23$.

The column was then saturated by imbibing Milli-Q water from the bottom of the column until there was flow at the top. Water was then pumped through the column from the bottom at 20 ml/hr for a minimum of 24 hr to help purge large air bubbles from the system. Saturation of the columns was verified by weighing the column after 24 hr. The saturation, θ_s , was calculated using Equation 4.3:

$$\theta_s = \frac{\left(\frac{\text{weight of water (g)}}{\rho_{\text{water}} \text{ (g/cm}^3\text{)}} \right)}{\left(\text{column volume (cm}^3\text{)} \right)(n)} \quad (4.3)$$

When the column weight was within $\pm 5\%$ of saturation, the flow was reversed to flow from the inlet to the outlet. The column was allowed to equilibrate for two pore volumes before the experiment was started.

After equilibration, approximately 400 ml (from five to six pore volumes) of the colloid suspension was pumped through the column at a rate of 20 ml/hr to allow the effluent concentration to reach equilibrium. For the first column experiment, the influent was then switched back to water for an additional 400 ml. The second column experiment was not flushed with water, and no further sampling was performed. The effluent was collected in 20-ml glass scintillation vials by an Isco Retriever IV fraction collector in 30-min intervals. The vials were weighed before and after the experiment to determine the total volume pumped through the column. The samples were then analyzed with the fluorometer at the excitation and emission wavelengths listed in Table 4.1.

Separate tracer experiments were run with a 10^{-3} -M potassium bromide (KBr) solution. The column was equilibrated as described above. An Accumet pH meter 50 (Fisher Scientific) was used to determine the KBr concentration. The Br⁻ and double junction reference electrodes were calibrated between 10^{-5} and 10^{-2} M KBr. The electrodes were then inserted into microflow cells attached to the column. The fluid contacted the double junction reference electrode first. The Br⁻ concentration was recorded to a printer in 15-min intervals. After breakthrough, the solution was switched to water until background was reached.

4.2.2 Unsaturated Column Experiments

Unsaturated column experiments were conducted in the Unsaturated Flow Apparatus (UFA), which is a modified ultracentrifuge (ASTM D18.21, 1996). Specifically, a modified Beckman J-6 ultracentrifuge and a HySed 3.0 rotor were used for these experiments. The rotor is specially designed to allow fluids to be pumped into the samples through two distinct fluid flow paths (Figure 4.7). The first is a central feed that pumps the fluid directly into the sample. The second is an annular feed around the central fluid path (Figure 4.8). The fluid is then passed through a dispersion cap to ensure a uniform moisture distribution to the sample.

The UFA and a similar apparatus have been used to measure hydraulic conductivity (Conca 1993, Nimmo et al. 1992, Nimmo et al. 1987), estimate recharge rates (Nimmo et al. 1994), study the movement of solutes in the vadose zone (Lindenmeier et al. 1995), and measure the hydraulic properties of carbon tetrachloride (Shields 1995). This study represents the first application of the UFA to colloid transport in porous media. No modifications had to be made to the centrifuge or the rotor, but changes in the experimental setup and operating procedure were necessary to study colloid transport. The major change was in the setup of the feed solution. The tubing used for the colloid suspension was Teflon, except for the pump bladder. The standard microinfusion pump bags were spliced. One injection port from the microinfusion pump bag was retained to remove air from the

line, if necessary. New pump bladders were used for every experiment even if the same suspension was used. The colloids have an affinity for the plastic in the pump bladder and will accumulate over time. The colloid suspension was stored in a glass container. It was then siphoned into the pump through the tubing rather than being gravity fed. The stock suspension was placed above the pumps to maintain a head gradient. These modifications were necessary to prevent the introduction of plasticizers and to prevent the colloids from sticking to the tubing.

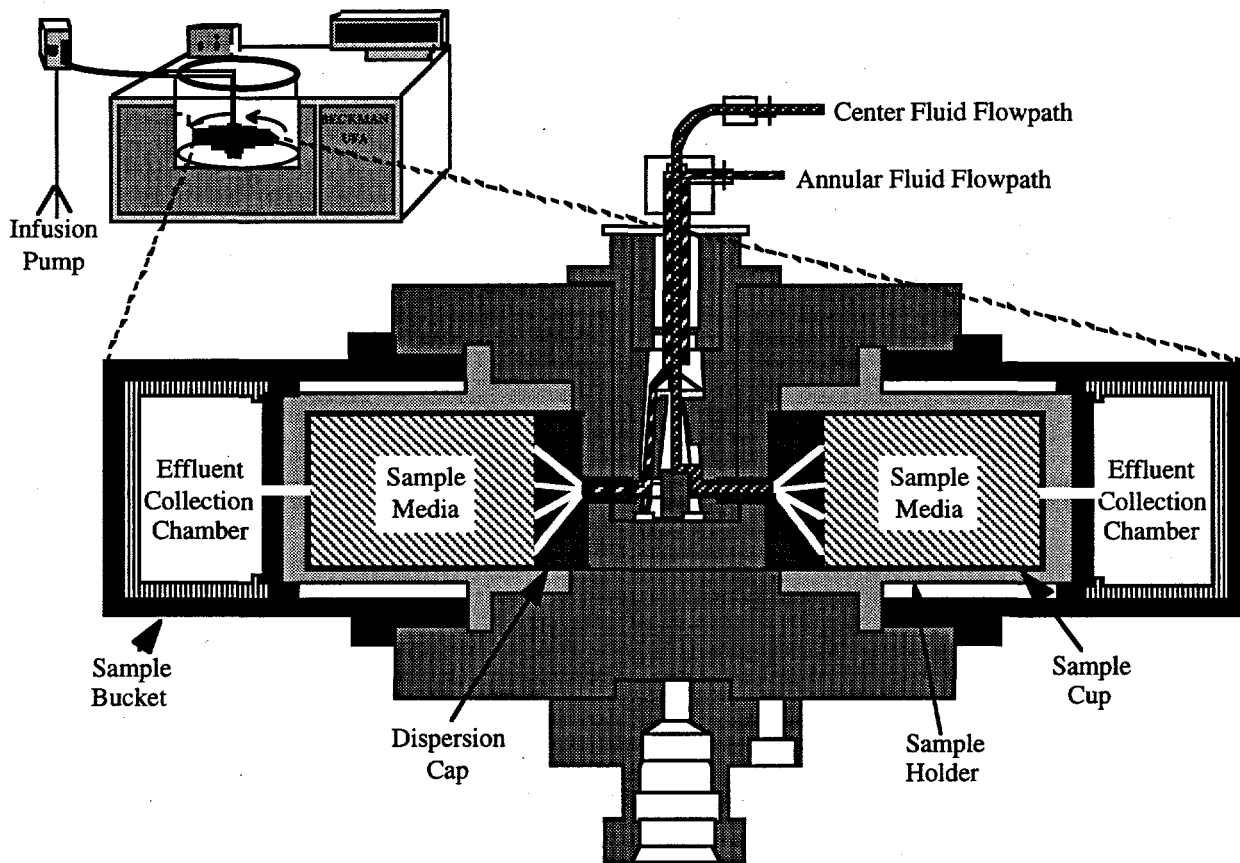


Figure 4.7. Schematic of UFA Rotor

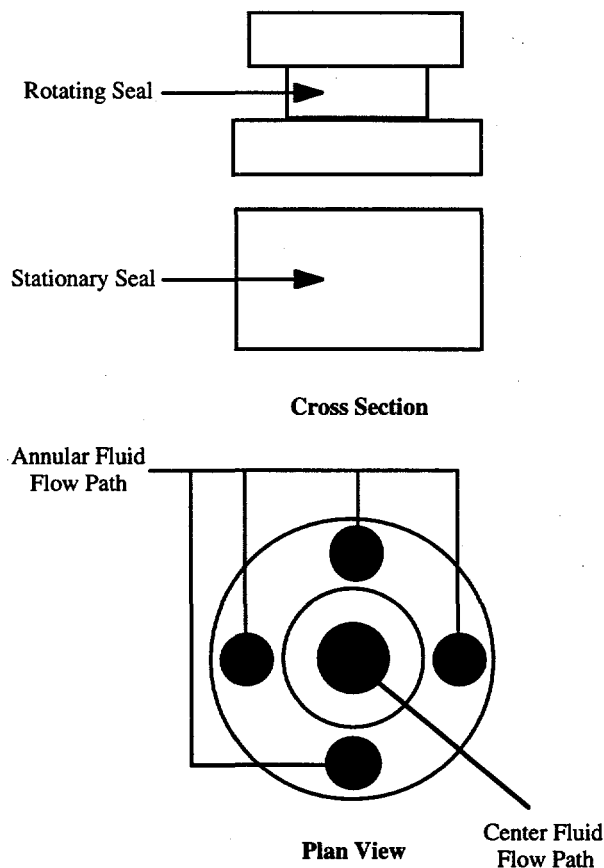


Figure 4.8. Schematic of UFA Face Seal

4.2.2.1 Theory of Flow in a Centrifuge

Fluid flow in the UFA is governed by Darcy's law, which states that the flux is equal to the hydraulic conductivity times the driving force. Assuming steady-state flow and neglecting gravity, this is represented as

$$q = -K(\psi) \left[\frac{d\psi}{dr} - \rho\omega^2 r \right], \quad (4.4)$$

where:

- | | |
|---|--|
| q = fluid flux (cm/s) | ρ = fluid density (gm/cm ³) |
| K = hydraulic conductivity (cm/s) | ω = rotation speed (radians/s) |
| r = distance from axis of rotation (cm) | ψ = matric potential. |

Ideal operation of the UFA occurs when the centrifugal driving force dominates the matric potential gradient, $\rho\omega^2 r \gg \frac{d\psi}{dr}$. For this system, this occurs when the rotation speed is greater than 300 rpm and there is sufficient flux density (Conca and Wright 1995). At this rate, the matric potential is negligible, which implies that θ is constant and $K(\theta)$ can be measured directly without measuring ψ (Nimmo et al. 1987). The equation now simplifies to

$$K(\theta) = \frac{q}{\rho \omega^2 r} \quad (4.5)$$

The θ -based form of this equation is applicable only to homogeneous unsaturated soils; for heterogeneous column experiments Equation 4.4 should be used. Unit analysis of this equation is

$$\frac{\text{cm}}{\text{s}} = \frac{\left(\frac{\text{cm}}{\text{s}}\right) \left(980.67 \frac{\text{g cm}}{\text{cm}^2 \text{cm}_{\text{H}_2\text{O}} \text{s}^2}\right)}{\left(\frac{\text{g}}{\text{cm}^3}\right) \left(\frac{1}{\text{s}^2}\right) (\text{cm})} \quad (4.6)$$

The right-hand term in the numerator converts the units from acceleration (g-force units) to a force-per-unit volume relative to water.

The advantage of the UFA technique is that the user can now control the hydraulic conductivity by manipulating the fluid flux and the rotation speed. At steady state the moisture distribution in the columns is uniform. This has been verified experimentally for soil, gravel, and sand columns (Conca and Wright 1994, Conca and Wright 1990, Nimmo et al. 1987).

4.2.2.2 Experimental Procedure

Different methods of sample preparation were tested before the experiments were conducted. It was found that for coarse sand the most consistent sample bulk density, ρ_b , was obtained through dry packing the column with a column vibrator. The sample holders were lined with filter paper and then weighed, and the value was recorded on the data sheet. The filter paper was then wetted with Milli-Q water and weighed. Next, sand was added in centimeter lifts, which were compacted with a column vibrator. This procedure was repeated until the column was packed. Size segregation was not a concern because of the uniform nature of the sand. The sample was then weighed to determine the dry weight of the sand added; this was done by subtracting the weight of the sample holder and wet filter paper. Unlike other UFA runs, where the dry sample weight can be determined after the experiment, in colloid experiments, where mass may be retained, it is crucial that the weight be determined before conducting the experiment. Next, the o-ring, plastic mesh cover, and dispersion cap were weighed and placed on the sample. The sample was then weighed again to verify the total weight of the sample.

Several basic parameters were calculated for each sample; these values were used in subsequent calculations. The porosity was calculated from Equation 4.1 and had a value of 0.41 ± 0.01 for the unsaturated experiments. The bulk density was calculated as

$$\rho_b = \frac{\text{dry sample weight (g)}}{\text{sample volume (cm}^3\text{)}} \quad (4.7)$$

The value for these experiments was $1.57 \pm 0.02 \text{ g/cm}^3$.

The next step was to saturate the sample on a falling-head apparatus. A modified burette was connected to the bottom of the sample holder. Milli-Q water was then flowed through the system to purge air bubbles and saturate the sample. Sample saturation was verified by weighing the entire sample assembly and subtracting the weight of the sample holder and filter paper. Saturation values slightly greater than 1.0 result from water being trapped in the sample lid. This introduces a slight

error, but it is very important not to disturb the sample after it has been packed. In early experiments, it was found that removing and replacing the lid caused spikes in the colloid concentration.

After the sample was saturated, falling-head measurements were made to estimate the saturated hydraulic conductivity (Klute and Dirksen 1986). The hydraulic conductivity was calculated as

$$K = \frac{aL}{At} \ln\left(\frac{H_1}{H_2}\right), \quad (4.8)$$

where

a	=	burette cross-sectional area	L	=	sample length
H ₁	=	initial water column height	H ₂	=	final water column height
A	=	sample cross-sectional area	t	=	time for water to fall from H ₁ to H ₂ .

The value from the falling-head measurement was used as the saturation point on the plot of hydraulic conductivity versus volumetric water content.

The first set of column experiments was used to determine the soil-water characteristic curve. Traditional laboratory methods, such as pressure plates, measure the volumetric water content against changes in pressure. This measurement is then related to the hydraulic conductivity through functional relationships (van Genuchten 1980). The UFA allows the relationship between K and θ to be measured directly.

The packed sand columns were placed in the metal sample holders lined with filter paper. For all the experiments, the temperature in the centrifuge was held constant at 23 ± 1 °C. The measurement of the soil-water characteristic curve was done on duplicate samples. The entire curve was not repeated for all samples because Nimmo and Akstin (1988) found that, for a sandy soil, K was accurate within $\pm 8\%$ at low moisture contents. Therefore, the initial runs were used to represent the general characteristics of the sand, and the individual data points from the column experiments were added to determine the variability between repacked columns.

To develop the curve, the samples were run at a fixed flow rate and rotation speed until they reached equilibrium. The sample holder with the lid in place was then weighed to determine the volumetric water content, which was calculated as

$$\theta = \left(\frac{\text{water content (g)}}{\text{dry sample weight}} \right) \frac{\rho_b}{\rho_w}. \quad (4.9)$$

Equation 4.5 was then used to calculate the hydraulic conductivity. The samples were then put back on the centrifuge at a higher rotation speed and/or lower flow rate to obtain $K(\theta)$ at a lower volumetric water content. This procedure was repeated until a wide range of hydraulic conductivities and volumetric water contents was determined. This information was then used to select the flow rate and rotation speed for the colloid experiments.

The desaturation data set was combined with the equilibrium data from the colloid experiments to create the characteristic curves for the sand. Figure 4.9 shows the variability of volumetric water content at specific values of hydraulic conductivity calculated by Equation 4.5. The error bars represent one standard deviation from the mean and indicate variability in the volumetric water content between column experiments. Some of the variability in the volumetric water content can be accounted for by hysteresis (Freeze and Cherry 1979). The samples were systematically desaturated to prevent instability, but during a single experiment the volumetric water content often fluctuated by

$\pm 10\%$, and the average value was used to represent the experiment. The majority of variation in volumetric water content is due to the differences between repacked columns. Different degrees of compaction alter the larger pore spaces, which are the first to drain at low moisture content. The smaller pores are not affected as much by the degree of compaction. This is consistent with what is observed in Figure 4.9. At low volumetric water contents, the variability between the repacked columns is small. As the volumetric water content increases, which relates to an increase in pore size, the variability between columns increases. The largest variability occurs at $K = 10^{-4}$ cm/s.

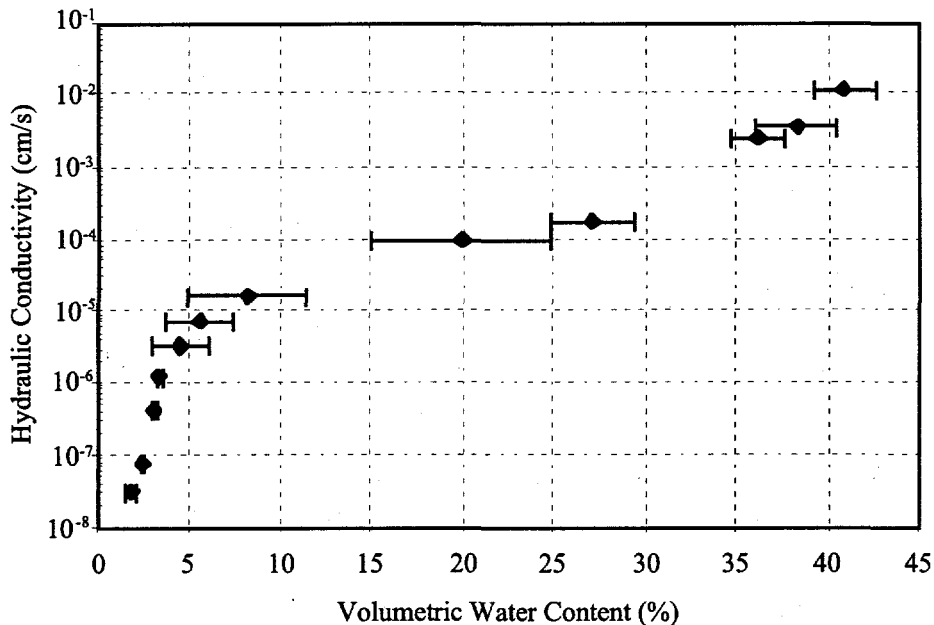


Figure 4.9. The Variability of the Volumetric Water Content Between the 90 Repacked Sand Columns Used in this Study. The values of hydraulic conductivity were fixed based on the flow rate (q) and rotation speed (ω). The error bars represent one standard deviation from the mean, or the amount of variability observed in the volumetric water content between columns at the same hydraulic conductivity.

Figure 4.10 shows the same data averaged to look at the variability in hydraulic conductivity. Unfortunately, the values of the volumetric water content were not the same for any of the experiments. Therefore, they were classified into groups of 1-2 units of volumetric water content. Appendix B contains a table of the data plotted and shows the standard deviation for the volumetric water content. The error bars in the figure represent the upper and lower values of the hydraulic conductivity. In contrast to Figure 4.9, the largest variability in hydraulic conductivity occurred at low volumetric water contents.

To understand the mechanisms for colloid transport, it is necessary to distinguish between entrapped air bubbles and a continuous gas phase in the column. The volumetric water content at which the gas phase becomes continuous depends on the matrix properties. According to capillary bundle theory, a porous medium can be thought of as a group of capillary tubes of different radii that represent a range of pore sizes (Jury et al. 1991). The volume of water in each capillary depends on changes in pressure, which is related to changes in the hydraulic conductivity and on the radii of the tube. At each incremental change in pressure the capillary tubes will start to drain, with the largest radii or largest pore spaces draining first. When a sufficient number of the large pore spaces have drained, the gas phase will become continuous. It is difficult to predict at what volumetric water

content this will occur. Based on Figures 4.9 and 4.10, the soil drains rapidly as the hydraulic conductivity decreases. It is assumed that when the volumetric water content is between 20% and 35% most of the large pore spaces have drained, which allows the gas phase to be continuous.

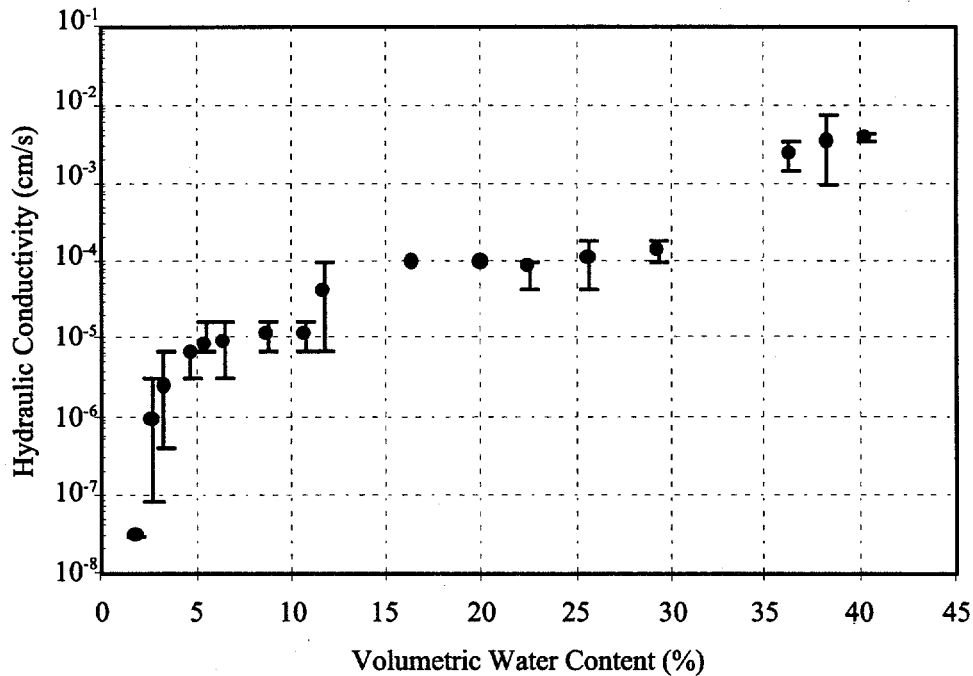


Figure 4.10. The Variability of the Hydraulic Conductivity Between the 90 Repacked Sand Columns Used in This Study. The values of volumetric content were averaged between one and two units. Each circle represents the average of 2 to 16 data points for both the volumetric water content and hydraulic conductivity. The error bars represent the high and low values of hydraulic conductivity.

Columns for colloid experiments were packed and saturated as described above. The sample was then equilibrated in the centrifuge at the desired flow rate and rotation speed. For these experiments, equilibrium was reached when the water content did not change by more than 0.1 gram during a 2-hr period. Then the Milli-Q water was changed to KBr or to the colloid suspension. The procedure for a KBr or colloid experiment is the same. The experiment was run according to the following procedure:

1. The water was drained from the rotor.
2. The room temperature colloid suspension was sonicated for a couple of minutes to ensure that the colloids were well dispersed and to remove air bubbles.
3. The flow lines were filled with the colloid suspension, with special care taken to ensure that no air bubbles were present in the line.
4. The colloid suspension was allowed to drain through the rotor for at least 1 min.

Table 4.4 shows the calculated values for the Stokes sedimentation velocity and specific discharge. At low volumetric water contents, where the angular velocity in the centrifuge was 1300 rpm, the specific discharge was the dominant velocity. For all the colloids except the 1900-nm, the Stokes sedimentation velocity was less than 2% of the specific discharge. For the 1900-nm colloids it was 28%, which indicates that the Stokes sedimentation velocity could have a significant affect on the experimental results. For gravity and angular velocities of 400 rpm, the sedimentation velocity for the different colloids sizes was <5% of the specific discharge. Therefore, the dominant force for colloid mobility is the advective force and not gravitational settling.

Table 4.4. Comparison of the Stokes Sedimentation Velocity and Specific Discharge for the Colloid Experiments

	$K = 7.46 \times 10^{-6} \text{ cm/s}$ ($\theta_{\text{avg}} = 7.9$)		$K = 1.03 \times 10^{-4} \text{ cm/s}$ ($\theta_{\text{avg}} = 20.11$)		$K \cong 1.16 \times 10^{-2} \text{ cm/s}$ (saturated)	
Colloid Size (nm)	Stokes Velocity (nm/s)	Specific Discharge (nm/s)	Stokes Velocity (nm/s)	Specific Discharge (nm/s)	Stokes Velocity (nm/s)	Specific Discharge (nm/s)
52	1.48×10^1	2.29×10^5	1.40×10^0	1.18×10^5	9.00×10^{-2}	2.83×10^3
189	1.96×10^2	2.91×10^5			1.19×10^0	2.83×10^3
545	1.63×10^3	1.68×10^5			9.89×10^0	2.83×10^3
910	4.54×10^3	2.78×10^5			2.76×10^1	2.83×10^3
1900	1.98×10^4	7.09×10^4			1.20×10^2	2.83×10^3

4.2.3.2 Effect of Rotation Speed on Colloid Transport in the UFA

As shown in Equation 4.5, the user can control the hydraulic conductivity by adjusting the flow rate and the rotation speed of the centrifuge. To test whether the rotation speed affects the transport of colloids, the hydraulic conductivity was held constant at $7.4 \times 10^{-6} \text{ cm/s}$ and the flow rate and rotation speed were adjusted. Three different combinations were examined: a) $\omega = 1100 \text{ rpm}$, $q = 26.9 \text{ ml/hr}$; b) $\omega = 1300 \text{ rpm}$, $q = 37.6 \text{ ml/hr}$; and c) $\omega = 1500 \text{ rpm}$, $q = 50 \text{ ml/hr}$. The hypothesis was that within experimental error, no difference would be observed in the transport of KBr and 189-nm colloids due to changes in rotation speed and flow rates. The columns were run in duplicate, with the same columns used for the KBr and colloid experiments at each speed.

The KBr tracer tests were done first for each sample. Figure 4.11 shows the results for the breakthrough and water flush of a 10^{-3} M KBr solution at the three different rotation speeds. The y-axis represents a normalized concentration, where the effluent concentration is divided by the influent concentration. The x-axis represents the number of pore volumes, which is the mass of water in grams, that were passed through the porous media. The "A" and "C" designations on the samples indicate the annular and central fluid feed positions on the rotor, respectively.

No trends were observed in the data with respect to rotation speed or flow rate for a conservative tracer. The coefficient of variation expresses the sample variability relative to the mean (Zar 1974) at specified pore volumes varied between 1% and 8%. These values were within experimental error. Therefore, no significant difference was found between the experiments. After the KBr concentration reached background levels, the samples were flushed for an additional hour to ensure removal of the salt before conducting the colloid experiments.

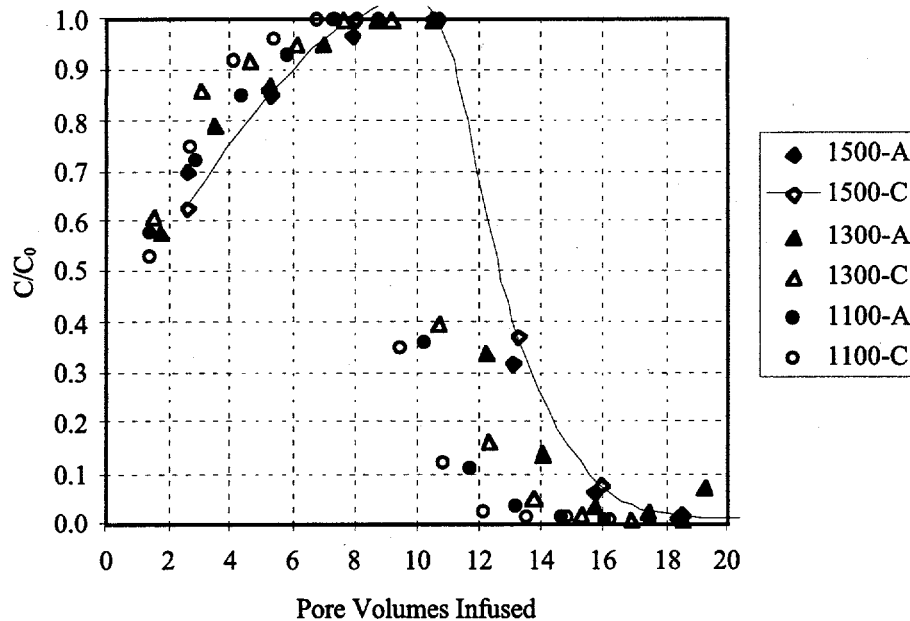


Figure 4.11. Breakthrough Curve of 10^{-3} M KBr at Different Flow Rates and Rotation Speeds to Determine if Changes in Rotation Speed Enhance Transport. The hydraulic conductivity was fixed at 7.4×10^{-6} cm/s. The water flush for each column started at a different pore volume. If the data are adjusted to start the water flush at the same pore volume, no difference is observed between the columns.

The colloid tests were done using 189-nm colloids. Figure 4.12 shows the results from the 189-nm colloid experiments at different rotation speeds and flow rates. No trend was observed for the data with respect to the rotation speed. For sample C at 1500 rpm, the breakthrough was significantly less than the other five experiments. The results from the KBr experiment on the same column lagged behind the other five experiments but was within experimental error (solid line in Figure 4.12). The lag in both the KBr and colloid experiment may indicate a problem with the column packing or obstruction in the sample holder and/or the dispersion cap. If the UFA enhanced the transport of colloids, it would be expected to be due to the increase in rotation speed. The results indicate that changes in the rotation speed did not enhance the transport of the colloids at a fixed hydraulic conductivity. Therefore, sample C at 1500 rpm is not included in the analysis to determine if there is a statistically significant difference between the experiments.

For the five experiments, seven pore volumes were selected for statistical analysis. Figure 4.13 shows the seven values used in the analysis. The solid line represents the average of the five data sets, and the dotted lines represent one standard deviation. The coefficient of variation at specific pore volumes was between 3% and 7%. It was also desirable to determine if the overall experimental results were different. A two-factor analysis of variance (ANOVA) was used to compare the five experiments. For the samples, $F=1.75 < F_{crit}=2.78$, which indicates that the null hypothesis of no significant difference between the samples is accepted. The p-value for the analysis was 0.17. For the results to be significantly different, the p-value must be ≤ 0.05 .

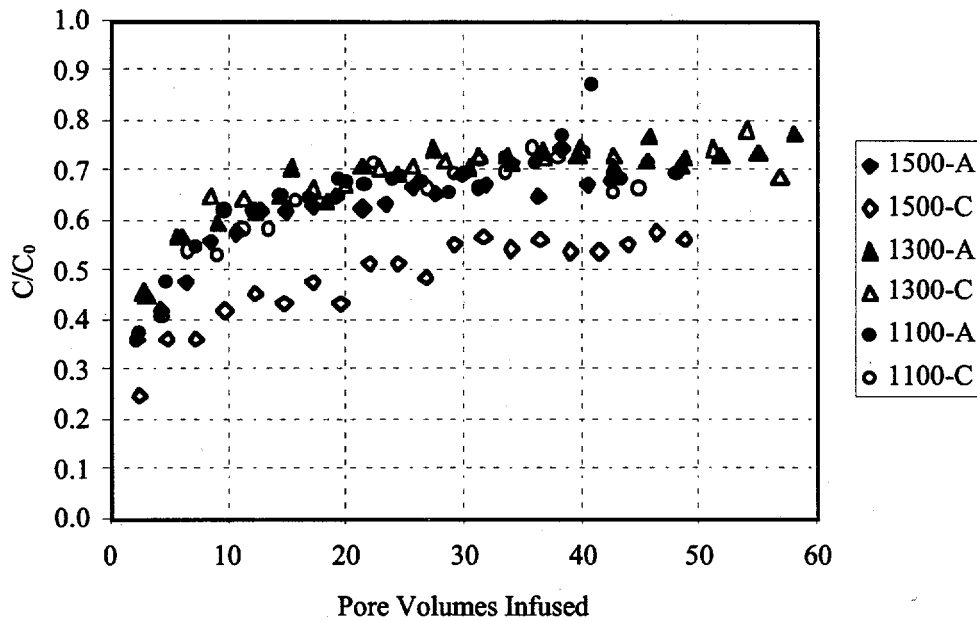


Figure 4.12. The Breakthrough of 189-nm Colloids at Different Flow Rates and Rotation Speeds to Determine if Changes in the Rotation Speed Enhances the Transport of Colloids. The hydraulic conductivity is fixed at 7.4×10^{-6} cm/s.

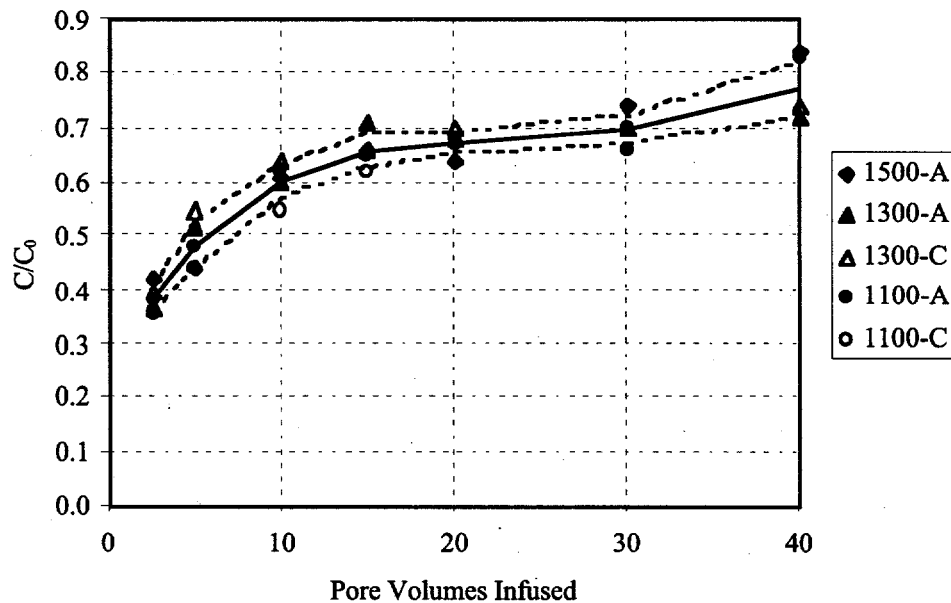


Figure 4.13. The Concentration Breakthrough of 189-nm Colloids Used in ANOVA Analysis to Test Whether the Rotation Speed Affects Colloid Transport. Seven points from Figure 4.12 were selected for the analysis. The solid line represents the average of five data sets and the dotted lines represent one standard deviation from the mean.

Figure 4.14 shows the cumulative percent mass recovered from the column, which represents an integration of the normalized concentration. The coefficient of variation for these data were between 3% and 7% at specified pore volumes. This analysis clearly indicates that within the $\pm 8\%$ experimental error, no significant difference was observed between the five colloid experiments at the three rotation speeds. Therefore, it was concluded that the UFA could be used to study the transport of colloids that have a density slightly greater than the feed solution.

4.3 Effect of Particle Size on Colloid Transport

In saturated porous media, the removal of colloidal particles due to filtration (physical straining) becomes significant when the ratio between the media diameter and the colloid diameter, d_m/d_c , < 20 (McDowell-Boyer et al. 1986). For unsaturated systems, the ratio may not be a sufficient indicator of when colloids will be retained. To examine other factors that influence colloid mobility and the effect of size on colloid transport, a series of experiments was conducted with a conservative tracer (KBr) and five different colloid sizes (52, 189, 545, 910, and 1900 nm). The experiments were run in duplicate under saturated and unsaturated conditions. The d_m/d_c ratio varied between 500 and 16,000 for these experiments, so particle retention would be due to chemical or physical mechanisms other than straining. For these experiments, chemistry does not play a critical role because the ionic strength of the solutions is very low, and both the sand and colloids are negatively charged.

Under partially saturated conditions, there are several potential physical retention sites, which are illustrated in Figure 4.15. Other physical mechanisms exist, such as gravitational settling, but are unlikely for the system being examined. The first retention site is colloid entrapment in the interstitial spaces between sand grains where the water flow is reduced or immobile. A second retention site would be for the colloid to become wedged between two grain surfaces and retained in the crevices. This is not the same as filtration, where the colloid is too large to fit through the pore throat. A third retention site is that the water film is too thin relative to the colloid size, which causes the colloids to become attached to the sand grains. It is unlikely that there would be sufficient buildup of colloids to cause filtration because the colloid concentration is dilute, and the capacity of the column to retain colloids is large. A final retention site would be for the colloidal particles to sorb on to an immobile gas bubble. This mechanism is more important at higher saturations when the gas phase is not continuous. Sorption to the air-water interface will be dependent on the ionic strength and the degree of hydrophobicity.

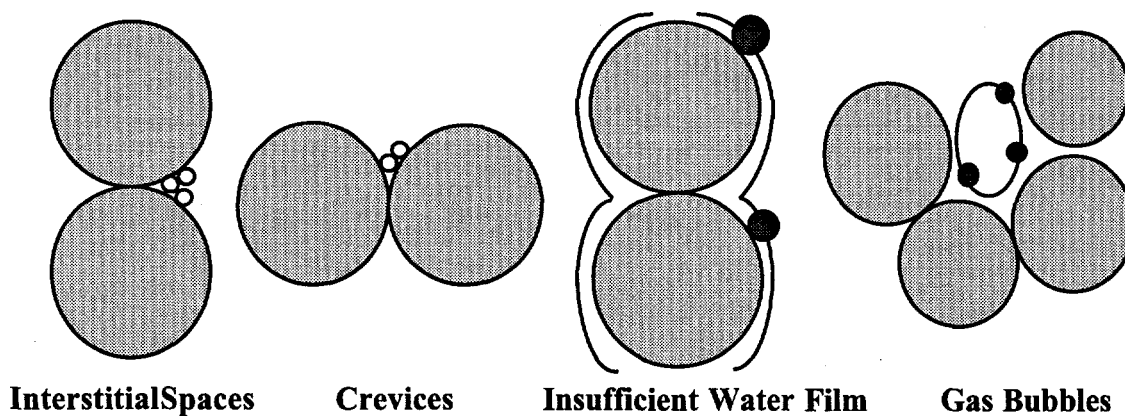


Figure 4.14. Possible Retention Sites for Mobile Colloids Through Porous Media Under Partially Saturated Conditions

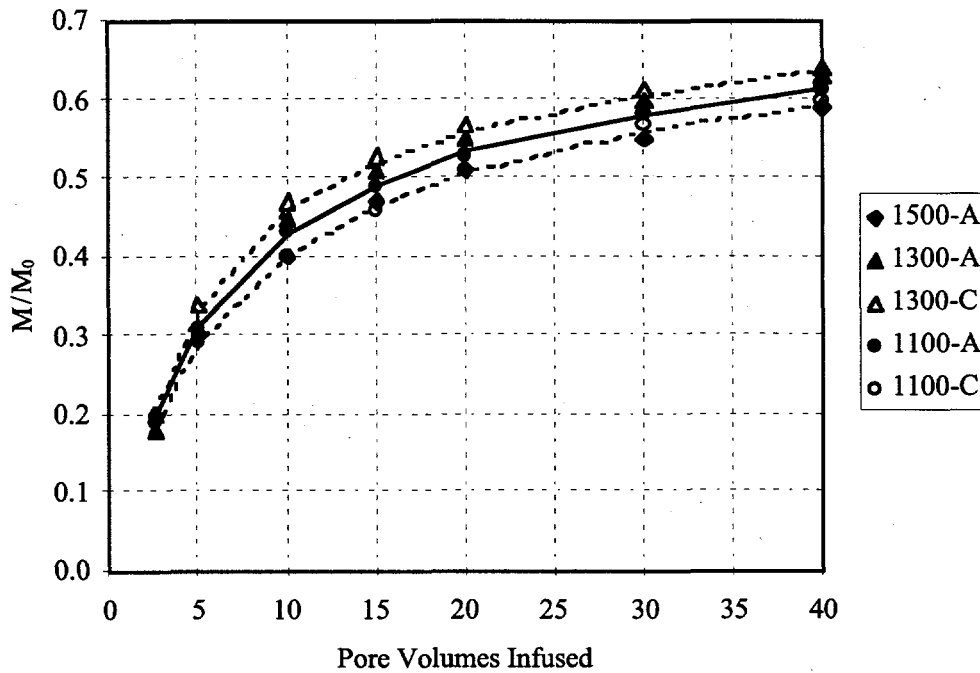


Figure 4.15. Cumulative Mass Recovery of 189-nm Colloids From the Column That was Used for Coefficient of Variation Analysis to Test if the Rotation Speed Affects Colloid Transport. The solid line represents the average of five data sets, and the dotted line represents one standard deviation from the mean.

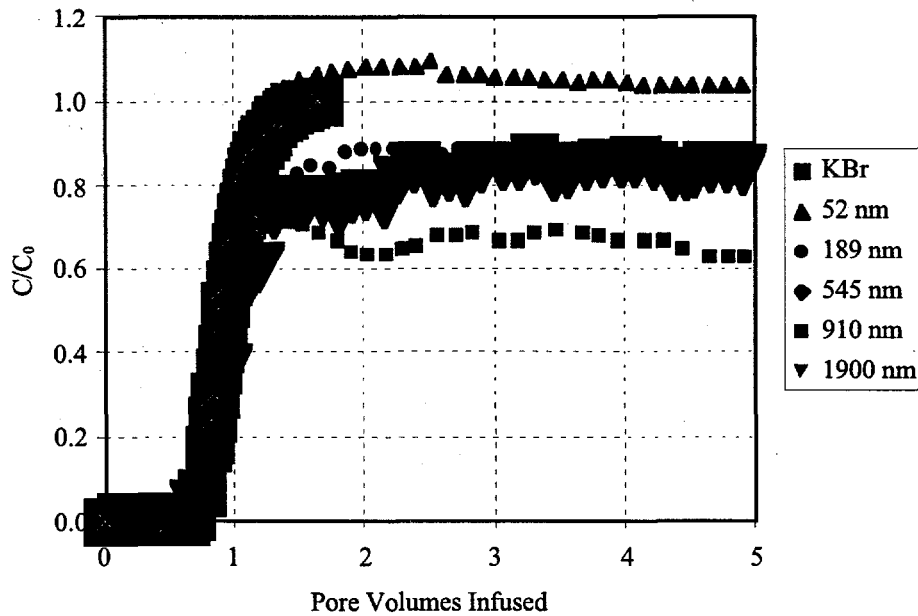


Figure 4.16. The Effect of Colloid Size on the Average Breakthrough of KBr and Latex Colloids Without Surface Functional Groups From Duplicate Experiments Under Saturated Conditions.

4.3.1 Saturated Column Experiments

The saturated colloid experiments were an upper boundary for colloid mobility. It was assumed that if the colloids were not mobile under saturated conditions they would not be mobile under partially saturated conditions. Figure 4.16 presents the average breakthrough for the KBr and the colloids from duplicate experiments. The normalized colloid concentration at 50%, $[C/C_0]_{50\%}$, occurred between 0.92 and 1.04 pore volumes, irrespective of size. This indicates that the colloids are not retarded relative to a conservative tracer, KBr, at this point in the experiment. The results of a single factor ANOVA on the pore volumes at $[C/C_0]_{50\%}$ shows that $F=0.93 < F_{crit}=4.39$, which indicates that there is no significant difference between the breakthrough of the colloids at $[C/C_0]_{50\%}$.

As the experiment progressed, the normalized concentration appeared to diverge for the different colloids. The 52-nm colloids, which were found to be hydrophilic based on contact angle measurements, fall on the same line as the KBr. This curve shows little dispersion and indicates that the KBr and the 52-nm colloids were not retained in the column. The normalized concentration breakthrough for the other colloids plateaus at lower concentrations. The plateau indicates that some of the colloids are being retained in the system, but that the matrix capacity for the colloids has not been exceeded.

The retention of the colloids could be due to sorption onto the matrix, diffusion, or dispersion into interstitial spaces or crevices. At the pH of the experiments, pH = 6.5-7.5, both the particles and the matrix have a negative charge, so electrostatic sorption is unlikely. To determine the extent of diffusion into interstitial spaces, the molecular diffusion coefficient was calculated from Equation 4.12 (de Marsily 1986):

$$d_0 = \frac{RT}{N} \frac{1}{6\pi\mu r_d}, \quad (4.12)$$

where

R = gas constant (J/K-mol)

μ = fluid viscosity (kg/m-s)

T = temperature (K)

N = Avogadro's number

r_d = radius of diffusing molecule (m).

This equation is applicable for dilute suspensions, and the value in porous media would be further reduced by an empirical constant that accounts for the matrix tortuosity (Freeze and Cherry 1979). The d_0 values for the 52-1900-nm colloids ranged from 8.23×10^{-10} to 2.25×10^{-11} m²/s, which resulted in colloid diffusions of less than 0.12 cm² during the 4 hr residence time. Therefore, the residence time of the colloids in the column is too short for diffusion to be a significant mechanism. Hence, the retention of the particles appears to be due to dispersion of the colloids into the interstitial spaces and/or crevices.

Before conclusions are drawn about the breakthrough of the different sized colloids, it is important to examine Figure 4.17, which shows the cumulative percent mass recovery for the same data set on the y-axis. The hump in the data around 5 pore volumes was from the solution being changed from the colloid suspension back to Milli-Q water. Based on the cumulative percent mass recovery, the 189, 545, 910, and 1900-nm colloids appeared to behave similarly during colloid infusion. During the water flush, the 910-nm colloid had a longer tail for the release of the colloids but still reached the 80-90% mass recovery range observed for all the other colloids, except the 52-nm colloid, which was completely recovered due to its hydrophilic nature and smaller size. This indicates that, for these saturated experiments, there is no size relationship for the 189, 545, 910, and 1900-nm colloids.

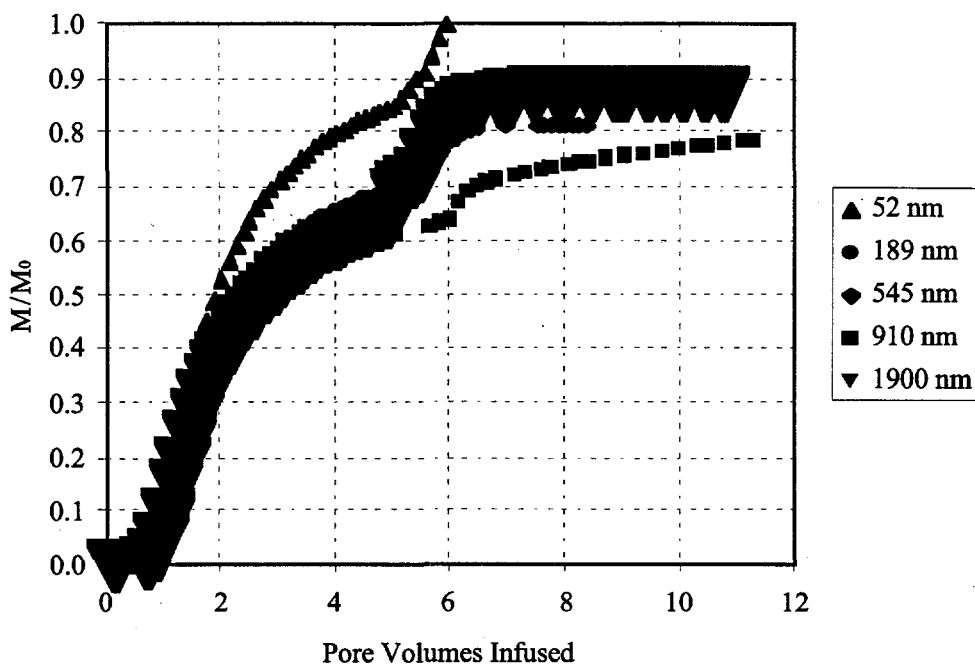


Figure 4.17. The Effect of Colloid Size on the Cumulative Percent Mass Recovered for KBr and Latex Colloids Without Surface Functional Groups From Duplicate Experiments Under Saturated Conditions.

4.3.2 Unsaturated Column Experiments

The unsaturated experiments were done at a fixed rotation speed and flow rate. The hydraulic conductivity was 7.4×10^{-6} cm/s, and the average volumetric water content was 6%. These conditions were selected to drive the system to the point where colloid transport would be inhibited. Figure 4.18 shows the concentration breakthrough for the unsaturated colloid experiments at $\theta_{\text{avg}} = 6\%$. For the KBr, the average $[C/C_0]_{50\%}$ was 1.35 pore volumes, which indicates that the breakthrough was retarded relative to the saturated KBr experiments, which had an average $[C/C_0]_{50\%}$ of 0.92 pore volumes. The colloid breakthrough occurred after the KBr for the 52 and 189-nm colloids, with the average $[C/C_0]_{50\%}$ equal to 1.75 and 3.78 pore volumes, respectively. The breakthrough of the 545, 910, and 1900-nm colloids did not reach $[C/C_0]_{50\%}$. Under partially saturated conditions, all of the colloids were retarded relative to the KBr.

Figure 4.19 shows the total mass recovery from the unsaturated experiments as a function of colloid size at $\theta_{\text{avg}} = 6\%$. There was an exponential decrease in the cumulative percent mass recovered as the colloid size increases. The correlation coefficient, R^2 , for the exponential function indicates that 98.91% of the variability in the cumulative percent mass recovered can be explained by the colloid size. These experiments used a coarse sand to minimize the effect of physical straining. The retardation of the colloids appears to be related to the volumetric water content, which varied

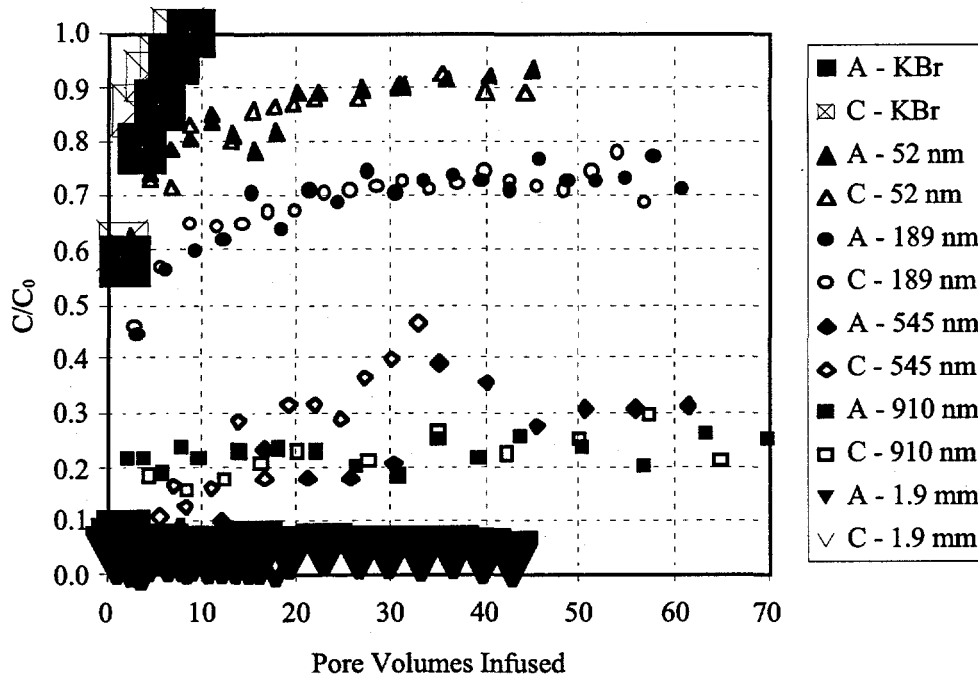


Figure 4.18. The Breakthrough of KBr and Latex Colloids Without Surface Functional Groups at $\theta_{avg} = 6\%$ to Examine the Effect of Size on Colloid Mobility.

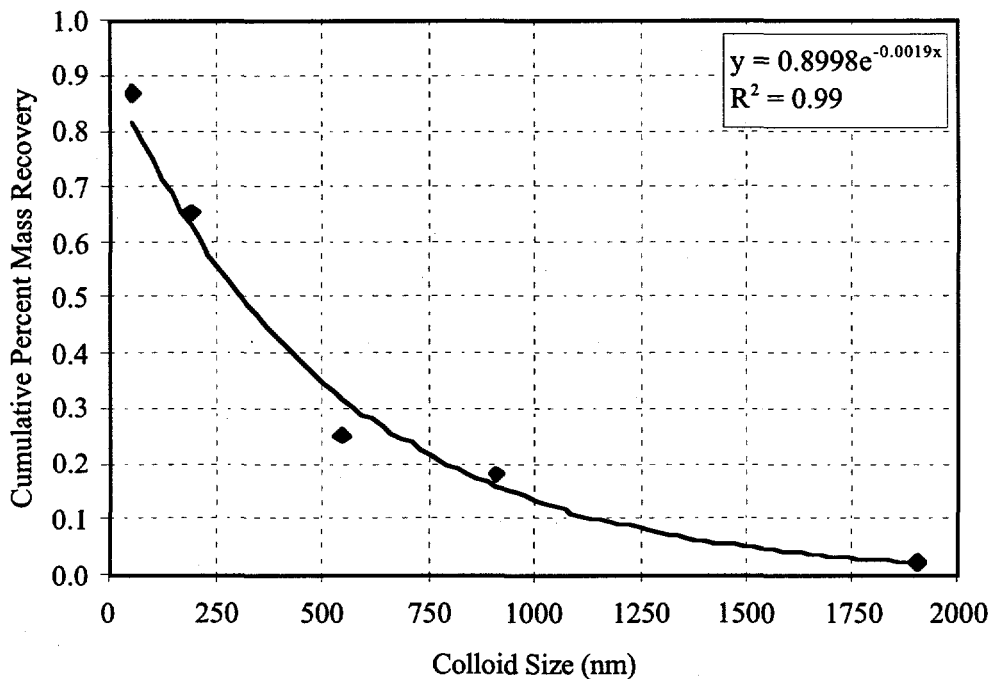


Figure 4.19. Cumulative Mass Recovered at 50 Pore Volumes for Latex Colloids Without Surface Functional Groups as a Function of Size at $\theta_{avg} = 6\%$. The solid line represents an exponential relationship between the percent recovered and colloid size.

between experiments. To normalize the data for these variations, the water film thickness (t_w) was calculated using Equation 4.13, which assumes that the water distribution around the sand grain was uniform (Mitchell 1993).

$$t_w = \frac{\theta}{\rho_b A_{ss}}, \quad (4.13)$$

where

θ = volumetric water content

ρ_b = density of sand (g/cm^3)

A_{ss} = specific surface area (cm^2/g).

Therefore, the value calculated provides an approximate value and does not account for local variations in the film thickness due to water meniscus between particles. In addition, the specific surface area for the sand was determined by the BET technique (Adamson 1990) on a Micrometrics 2000. In these experiments, $\theta_{\text{avg}} = 6\%$, $\rho_b = 1.57 \text{ g/cm}^3$, and the specific surface area was $0.3363 \text{ m}^2/\text{g}$, which resulted in an average t_w of 114 nm.

Figure 4.20 illustrates the different colloid sizes in proportion to the water film thickness. For small colloids, such as the 52-nm, the colloids are so small relative to the water film thickness that even if they were present as doublets or triplets they would be unlikely to be retarded. Hydrophobic colloids less than or equal to the water film thickness will be mobile along the air-water interface. Larger colloids will be retarded due to frictional forces between the colloids and the matrix.

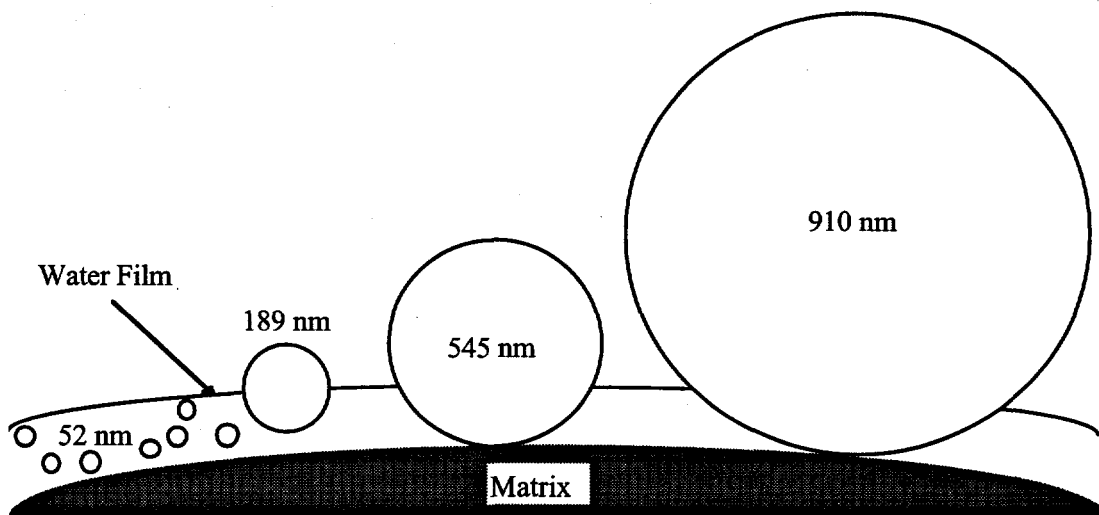


Figure 4.20. Proportional Schematic of Different Sized Colloids Without Surface Functional Groups in a 114-nm Water Film ($\theta_{\text{avg}} = 6\%$)

The ratio of the water film thickness to the colloid size indicates how many colloids or what portion of the colloid fits within the water film. In Figure 4.21, the ratio was plotted against the cumulative percent mass recovered after 50 pore volumes. For the hydrophobic colloids, the cumulative percent mass recovered decreased linearly with colloid size ($y = 2.70x - 0.41$, $R^2 = 1.00$), which is consistent with the schematic presented in Figure 4.20. The cumulative percent mass recovered for the 52 and 910-nm colloids was higher than would have been predicted for hydrophobic colloids. This provides the first verification of the contact angle measurements that indicated the colloids were indeed hydrophilic (Table 4.2).

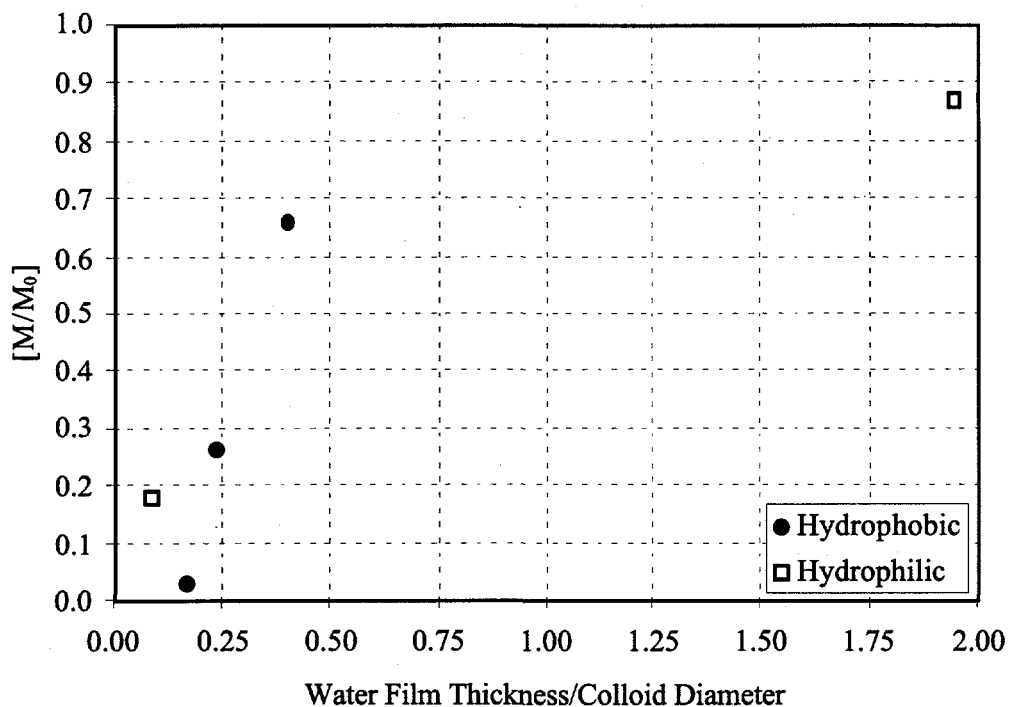


Figure 4.21. Cumulative Percent Mass Recovery at 50 Pore Volumes for Latex Colloids Without Surface Functional Groups as a Ratio of the Water Film Thickness/Colloid Size. The ratio indicates the number of colloids or the portion of colloids that can fit within the water film.

4.3.3 Discussion

For colloid transport to be an important mechanism for contaminant transport in the unsaturated zone, a significant portion of the colloids must be mobile at low moisture contents. These experiments have shown that the colloids are mobile under steady-state conditions, but it is difficult to determine what constitutes a significant mass of colloids. If a contaminant that sorbs to colloids is highly toxic at low concentrations, then the transport of 5-10% of the colloids may be considered significant. However, it must also be noted that the percentage of colloids that serve as carriers will also vary based on the affinity between the contaminants and the colloids (Kaplan et al. 1995).

These experiments were conducted in a simplified system and did not include filtration or increases in ionic strength that would further reduce colloid mobility. If the critical M/M_0 for a study site was determined to be 50%, then based on the equation in Figure 4.19, the colloid size necessary to meet this criteria at 6% volumetric water content is 325 nm. This value was used to select the colloid sizes for the second set of experiments, which examine the differences between hydrophobic and hydrophilic colloids.

5.0 Conclusion

The objectives of this study were to evaluate three aspects of colloid-facilitated transport of radionuclides as they specifically relate to the LLW-PA. These objectives were to:

1. Determine if the chemical conditions likely to exist in the near and far field of the proposed disposal site are prone to induce flocculation (settling of colloids from suspension) or dispersion of naturally occurring Hanford colloids
2. Identify the important mechanisms likely involved in the removal of colloids through a Hanford sediment
3. Determine if colloids can move through unsaturated porous media.

A series of batch experiments were conducted to identify the chemical conditions for which dispersion and flocculation (settling out of suspension) of Hanford sediment colloids (<1000 nm) would occur. These experiments determined the CFC, the minimum electrolyte concentration to induce colloids to flocculate from suspension. These CFC values were calculated for a range of sodium concentrations and pH values that may exist in the near and far fields. These groundwater parameters are considered to be among the most important parameters affecting colloid suspension stability. The experiments suggest that natural Hanford groundwater is not likely to maintain colloids in suspension. This in turn suggests that little or no mobile colloids are likely to exist in natural Hanford sediments. Specifically, the electrolyte concentration (9.86 mmol/L) of the groundwater is sufficiently high for the relatively low sodium concentrations (SAR = 1.04) and pH (8.1) conditions existing in Hanford groundwater to induce colloid flocculation. Chemical conditions in the near field also are not likely to be conducive for maintaining colloids in suspension. Even fewer suspended colloids are predicted to exist in the near field than in the far field. This was a somewhat unexpected result because preliminary calculations indicate that the pH (pH = 10) and sodium concentrations (0.5 M Na, SAR = 19,514 [mmol/L]^{0.5}) may be quite high in the near field, conditions conducive to colloid dispersion. However, the electrolyte concentration (1090 mmol/L) in the plume will concomitantly increase with the pH and sodium to sufficiently high levels that colloid flocculation would be expected.

Simulations of colloid removal by saturated porous media were conducted. These simulations were based on filtration theory, a semi-empirical model that explicitly attributes colloid removal to diffusion (Brownian motion), electrostatic attraction (colloid/colloid and colloid/sediment), gravitational settling, and interception (sieving). These simulations indicated that colloids with diameters between 200 and 500 nm were the most likely to move through sandy-textured sediments. Below this range, colloids were removed from suspension by diffusional, followed by adsorption, processes. Above this range, colloids were removed from suspension by gravitational settling. Mobile colloid sizes reported in the literature are essentially always in this size range, providing additional credence to these results. One important implication of this finding is that even if a suspension of nanometer-size colloids were formed from the waste form (such as colloidal radionuclide precipitates), they would likely be retained by the sediment as a result of diffusional removal processes.

These simulations also indicate that colloid removal by sediments was not sensitive to flow rate, but was sensitive to colloid size and sediment particle size. Throughout the wide range of conditions evaluated, colloid removal by gravitational settling and diffusion were appreciably more important than electrostatic and interception (sieving) processes.

Experiments were also conducted to determine if colloids could move through unsaturated conditions. This issue is experimentally difficult to evaluate. The approach taken in this series of studies was to use an extremely well controlled and defined system. The system consisted of water, uniformly sized sand, and fluorescent latex colloids. The degree of saturation in the sand columns were carefully controlled using a UFA. The effect of colloid size (from 52 to 1900 nm) and degree of saturation (from 6 to 100%) on colloid transport were investigated. These experiments simulated a system in which colloids were already formed and were highly dispersive (would not flocculate from suspension). Under saturated conditions, the amount of colloids removed from suspension did not vary as a function of colloid size. However, in unsaturated conditions, colloid size did have a profound effect on colloid transport. At 6% volumetric water content, approximately the degree of saturation expected in the Hanford vadose zone, colloid removal increased exponentially as colloid size increased. It was proposed that the decrease in colloid mobility at low volumetric contents was due to the colloids being dragged along the sand grain and retarded as the ratio between the water film thickness and colloid size decreased. The most mobile colloids at 6% water content were less than 60 nm.

In conclusion, these studies suggest that if colloids containing radionuclides (radiocolloids) are present, the groundwater chemistry in the near and far fields likely will cause them to flocculate. This would preclude colloid facilitated transport of radionuclides from the disposal site. In the event that radiocolloids are in fact stable in groundwater, only the smallest of colloids, <60-nm in diameter, would be able to move through the unsaturated vadose zone. The larger colloids would be retained by the sediment. If these <60-nm radionuclides reached the aquifer, i.e., the saturated zone, they likely would be removed from the groundwater by diffusional processes.

6.0 References

- Adamson, A. W. 1990. *Physical Chemistry of Surfaces*, John Wiley and Sons, Inc., New York.
- Amrhein, C., P. A. Mosher, and J. E. Strong. 1993. "Colloid-Assisted Transport of Trace Metals in Roadside Soils Receiving Deicing Salts." *Soil Sci. Soc. Am. J.*, 57(5):1212-1217.
- Backhus, D. A., J. N. Ryan, D. M. Groher, J. K. MacFarlane, and P. M. Gschwend. 1993. "Sampling Colloids and Colloid-Associated Contaminants in Ground Water." *Ground Water*, 31(3):466-479.
- Ballard, T. M. 1971. "Role of Humic Carrier Substances in DDT Movement Through Forest Soil." *Soil Sci. Soc. Amer. Proc.*, 35, 145-147.
- Bates, J. K., J. P. Bradley, A. Teetsov, C. R. Bradley, and B. M. Buchholtzen. 1992. "Colloid Formation During Waste Form Reaction: Implications for Nuclear Waste Disposal." *Science*, 256:649-651.
- Bertand, A. R., and K. Sor. 1962. "The Effects of Rainfall Intensity on Soil Structure and Migration of Colloidal Materials in Soils." *Soil Sci. Soc. Proc.*, 297-300.
- Birkeland, P. W. 1984. *Soils and Geomorphology*. Oxford University Press, New York.
- Buck, E. C., J. K. Bates, J. C. Cunnane, W. L. Ebert, X. Geng, and D. J. Wronkiewicz. 1993. "Analytical Electron Microscopy Study of Colloids from Nuclear Waste Glass." *Mat. Res. Soc. Symp. Proc.*, 294:199-206.
- Buddemeier, R. W., and J. R. Hunt. 1988. "Transport of Colloidal Contaminants in Groundwater: Radionuclide Migration at the Nevada Test Site." *Applied Geochemistry*. 3:535-548.
- Champ, D. R., J. L. Young, D. E. Robertson, and K. H. Abel. 1984. "Chemical Speciation of Long-lived Radionuclides in a Shallow Groundwater Flow System." *Water Pollution Res. J. Canada*. 19:35-54.
- Chen, Y., B. P. McGrail, and D. W. Engel. 1997. "Source-Term Analysis for Hanford Low-Activity Tank Waste Using the Reaction-Transport Code ARESY-CT." *Scientific Basis for Nuclear Waste Management XX*. W. C. Gray and I. Tray (Eds), Materials Research Society, Pittsburgh.
- Conca, J. L. 1993. *Measurement of Unsaturated Hydraulic Conductivity and Chemical Transport in Yucca Mountain Tuff*. LA-12596-MS, Los Alamos National Laboratory, Los Alamos, New Mexico.
- Conca, J. L., and J. Wright. 1990. "Diffusion Coefficients in Gravel Under Unsaturated Conditions." *Water Resour. Res.*, 26(5):1055-1066.
- Conca, J. L., and J. Wright. 1994. "The UFA Technology for Characterization of In-Situ Barrier Materials." *The 33rd Hanford Symposium on Health and Environment*, Pasco, Washington, 1179-1193.
- Conca, J. L., and J. Wright. 1995. "A New Technology for Determining Transport Parameters in all Porous Media." *Proceedings of the American Nuclear Society Topical Meeting on Mathematics and Computations, Reactor Physics, and Environmental Analyses*, Portland, Oregon.

- Degueudre, C., G. Longworth, V. Moulin, and P. Vilks. 1989. *Grimsel Colloid Exercise. An International Intercomparison Exercise on the Sampling and Characterization of Groundwater Colloids*. Paul Scherrer Institut-Bericht Nr. 39, Wurenlingen und Villigen, Switzerland.
- de Marsily, G. 1986. *Quantitative Hydrogeology-Groundwater Hydrology for Engineers*, Gunilla de Marsily, translator, Academic Press, Orlando, Florida.
- Dunnivant, F. M., P. M. Jardine, D. L. Taylor, and J. F. McCarthy. 1992. "Transport of Naturally Occurring Dissolved Organic Carbon in Laboratory Columns Containing Aquifer Material." *Soil Sci. Soc. Am. J.*, 56(2):437-444.
- Elimelech, M., and C. R. O'Melia. 1990. "Kinetics of Deposition of Colloidal Particles in Porous Media." *Environ. Sci. Technol.* 24:1528-1536.
- Enfield, C. G., G. Bengtsson, and R. Lindqvist. 1989. "Influence of Macromolecules on Chemical Transport." *Environ. Sci. Technol.*, 23(10):1278-1286.
- Feng, X., E. C. Buck, C. Mertz, J. K. Bates, and J. C. Cunnane. 1993. "Study on the Colloids Generated from Testing of High-Level Nuclear Waste Glass." *Proceedings of the Symposium on Waste Management*, Tuscon, Arizona, February 28 - March 4, 1993, 2:1015-1021.
- Freeze, R. A., and J. A. Cherry. 1979. *Groundwater*, Prentice Hall, Inc., Englewood Cliffs, New Jersey.
- Frenkel, H., J. O. Goertzen, and J. D. Rhoades. 1978. "Effects of Clay Type and Content, Exchangeable Sodium Percentage, and Electrolyte Concentration on Clay Dispersion and Soil Hydraulic Conductivity." *Soil Sci. Soc. Am. J.*, 42:32-39.
- Gee, G. W., and J. W. Bauder. 1986. "Particle-size Analysis." In: *Methods of Soil Analysis, Part 1, Physical and Mineralogical Methods, Second Edition*, A. Klute, Ed., American Society of Agronomy, Madison, Wisconsin, 383-412.
- Goldberg, S., and H. S. Forster. 1990. "Flocculation of Reference Clays and Arid-Zone Soil Clays." *Soil Sci. Soc. Am. J.*, 54:714-718.
- Goldenberg, L. C., I. Hutcheon, and N. Wardlaw. 1989. "Experiments on Transport of Hydrophobic Particles and Gas Bubbles in Porous Media." *Transport in Porous Media*, 4:129-145.
- Gounaris, V., P. R. Anderson, and T. M. Holsen. 1993. "Characteristics and Environmental Significance of Colloids in Landfill Leachate." *Environ. Sci. Technol.*, 27(7):1381-1387.
- Greene, M. R., D. A. Hammer, and W. L. Olbricht. 1994. "The Effect of Hydrodynamic Flow on Colloidal Stability." *J. Colloid Interface Sci.*, 167:232-246.
- Gschwend, P. M., and M. D. Reynolds. 1987. "Monodisperse Ferrous Phosphate Colloids in an Anoxic Groundwater Plume." *J. Contam. Hydrol.* 1: 309-327.
- Gschwend, P. M., D. A. Backhus, J. K. MacFarlane, and A. L. Page. 1990. "Mobilization of Colloids in Groundwater Due to Infiltration of Water at a Coal Ash Disposal Site." *J. Contam. Hydrol.*, 6, 307-320.
- Hartman, M. J., and P. E. Dresel. 1997. *Hanford Site Groundwater Monitoring for Fiscal Year 1996*. PNNL-11470. Pacific Northwest National Laboratory, Richland, Washington.

- Harvey, R. W., L. H. George, R. L. Smith, and D. R. LeBlanc. 1989. "Transport of Microspheres and Indigenous Bacteria Through a Sandy Aquifer: Results of Natural and Forced Gradient Tracer Experiments." *Environ. Sci. Technol.*, 23:51-56.
- Herzig, J.P., D.M. Leclerc, and P. Le Goff. 1970. "Flow of Suspensions Through Porous Media - Application to Deep Filtration." *Indust. Engineer. Chem.* 62:8-35.
- Higgo, J. J. W., G. M. Williams, and I. Harrison. 1993. "Colloid Transport in a Glacial Sand Aquifer - Laboratory and Field Studies." *Colloids and Surfaces A: Physicochemical and Engineering Aspects*, 3:179-200.
- Ho, C. H., and N. H. Miller. 1986. "Formation of Uranium Oxide Sols in Bicarbonate Solutions." *J. Colloid Interface Sci.*, 113:232-240.
- Jardine, P. M., G. V. Wilson, J. F. McCarthy, R. J. Luxmoore, D. L. Taylor, and L. W. Zelazny. 1990. "Hydrogeochemical Processes Controlling the Transport of Dissolved Organic Carbon Through a Forested Hillslope." *J. Contam. Hydrol.*, 6:3-19.
- Jury, W. A., W. R. Gardner, and W. H. Gardner. 1991. *Soil Physics*, John Wiley and Sons, Inc., New York.
- Kan, A. T., and M. B. Tomson. 1990. "Ground Water Transport of Hydrophobic Organic Compounds in the Presence of Dissolved Organic Matter." *Environ. Toxicol. Chem.*, 2:253-263.
- Kaplan, D. I., P. M. Bertsch, and D. C. Adriano. 1995. "Facilitated Transport of Metals Through an Acidified Coastal Plain Aquifer." *Ground Water* 33:708-717.
- Kaplan, D. I., P. M. Bertsch, and D. C. Adriano. 1997 (in press). "Mineralogical and Physico-Chemical Differences Between Mobile and Nonmobile Colloidal Phases in Ultisol Pedons." *Soil Sci. Soc. Am. J.*
- Kaplan, D. I., P. M. Bertsch, D. C. Adriano, and W. P. Miller. 1993. "Soil-Borne Mobile Colloids as Influenced by Water Flow and Organic Carbon." *Environ. Sci. Technol.* 27:1193-1200.
- Kaplan, D. I., P. M. Bertsch, D. C. Adriano, and K. A. Orlandini. 1994. "Actinide Association with Groundwater Colloids as a Function of Distance from a Point Source." *Radiochimica Acta* 66/67:181-187.
- Kaplan, D. I., K. J. Cantrell, T. W. Wietsma, and M. A. Potter. 1996a. "Retention of Zero-Valent Iron Colloids by Sand Columns: Application to Chemical Barrier Formation." *J. of Environ. Quality*. 25:1086-1094.
- Kaplan, D. I., R. J. Serne, A. T. Owens, J. L. Conca, T. W. Wietsma, and T. L. Gervais. 1996b. "Radionuclide Adsorption Distribution Coefficients Measured in Hanford Sediments for the Low Level Performance Assessment Project." PNNL-11385, Pacific Northwest National Laboratory, Richland, Washington.
- Kaplan, D. I., M. E. Sumner, P. M. Bertsch and D. C. Adriano. 1996c. "Chemical Conditions Conducive to the Release of Mobile Colloids from Ultisol Profiles." *Soil Sci. Soc. Am. J.* 60:269-274.
- Kia, S. F., H. S. Fogler, and M. G. Reed. 1987. "Effect of pH on Colloidally Induced Fines Migration." *J. Colloid Interface Sci.*, 118(1):158-168, 1987.

Kim, J. I., W. Treiber, C. Lierse, and P. Offerman. 1985. "Solubility and Colloid Generation of Plutonium from Leaching of HLW Glass in Salt Solutions." *Mat. Res. Soc. Symp. Proc.*, 44:359-369.

Klute, A., and C. Dirksen. 1986. "Hydraulic Conductivity and Diffusivity: Laboratory Measurements." In: *Methods of Soil Analysis, Part 1, Physical and Mineralogical Methods*, A. Klute, Ed., American Society of Agronomy, Madison, 687-734.

Lindenmeier, C. W., R. J. Serne, J. L. Conca, A. T. Owen, and M. I. Wood. 1995. *Solid Waste Leach Characteristics and Contaminant-Sediment Interactions Volume 2: Contaminant Transport under Unsaturated Moisture Contents*. PNL-10722, Pacific Northwest Laboratory, Richland, Washington.

Magaritz, M., A. J. Amiel, D. Ronen, and M. C. Wells. 1990. "Distribution of Metals in a Polluted Aquifer: A Comparison of Aquifer Suspended Material to Fine Sediments of the Adjacent Environment." *J. Contam. Hydrol.*, 5:333-347.

Mann, R. M., C. R. Eiholzer, A. H. Lu, P. D. Rittman, N. W. Kline, Y. Chen, B. P. McGrail, G. F. Williamson, and N. R. Brown. 1996. *Hanford Low-Level Tank Waste Interim Performance Assessment*. WHC-EP-0884. Westinghouse Hanford Company, Richland, Washington.

McCarthy, J. F., and C. Degueldre. 1993. "Sampling and Characterization of Colloids and Particles in Groundwater for Studying Their Role in Contaminant Transport." In: *Environmental Particles*, J. Buffle and H. P. van Leeuwen, Eds., Lewis Publishers, Boca Raton, Florida.

McCarthy, J. F., and B. D. Jimenez. 1985. "Interactions Between Polycyclic Aromatic Hydrocarbons and Dissolved Humic Material: Binding and Dissociation." *Environ. Sci. Technol.*, 19(11):1072-1076.

McCarthy, J. F., T. M. Williams, L. Liang, P. M. Jardine, L. W. Jolley, D. L. Taylor, A. V. Palumbo, and L. W. Cooper. 1993. "Mobility of Natural Organic Matter in a Sandy Aquifer." *Environ. Sci. Technol.*, 27:667-676.

McCarthy, J. R., and J. M. Zachara. 1989. "Subsurface Transport of Contaminants." *Environ. Sci. Technol.* 23:496-502.

McDowell-Boyer, L. N., J. R. Hunt, N. Sitar. 1986. "Particle Transport Through Porous Media." *Water Resour. Res.*, 2:1901-1921.

Means, J. C., and R. Wijayarante. 1982. "Role of Natural Colloids in the Transport of Hydrophobic Pollutants." *Science*, 215:968-970.

Miller, W. P., H. Frenkel, and K. D. Newman. 1990. "Flocculation Concentration and Sodium/Calcium Exchange of Kaolinitic Soil Clays." *Soil Sci. Soc. Am. J.*, 54(2):346-351.

Mitchell, J. K. 1993. *Fundamentals of Soil Behavior*, John Wiley and Sons, Inc., New York.

Nightingale, H. I., and W. L. Bianchi. 1977. "Ground-Water Turbidity Resulting from Artificial Recharge." *Ground Water*, 15:146-152.

Nimmo, J. R., J. Rubin, and D. P. Hammermeister. 1987. Unsaturated Flow in a Centrifugal Field: Measurements of Hydraulic Conductivity and Testing of Darcy's Law. *Water Resour. Res.*, 23(1):124-134.

- Nimmo, J. R., and K. C. Akstin. 1988. "Hydraulic Conductivity of a Sandy Soil at Low Water Content After Compaction by Various Methods." *Soil Sci. Soc. Am. J.*, 52(2):303-310.
- Nimmo, J. R., K. C. Akstin, and K. A. Mello. 1992. "Improved Apparatus for Measuring Hydraulic Conductivity at Low Water Content." *Soil Sci. Soc. Am. J.*, 56(6):1758-1761.
- Nimmo, J. R., D. A. Stonestrom, and K. C. Akstin. 1994. "The Feasibility of Recharge Rate Determination Using the Steady-State Centrifuge Method." *Soil Sci. Soc. Am. J.*, 58:49-56.
- O'Melia, C. R. 1987. "Colloids in Aquatic Systems." *Aquatic Surface Chemistry: Chemical Processes at the Particle-Water Interface*. W. Stumm, Ed., Wiley Interscience. New York, 385-401.
- Penrose, W. R., W. L. Polzer, E. H. Essington, D. M. Nelson, and K. A. Orlandini. 1990. "Mobility of Plutonium and Americium Through a Shallow Aquifer in a Semiarid Region." *Environ. Sci. Technol.* 24:228-234.
- Powelson, D. K., J. R. Simpson, and C. P. Gerba. 1990. "Virus Transport and Survival in Saturated and Unsaturated Flow Through Soil Columns." *J. Environ. Qual.*, 19(3):396-401.
- Puls, R. W. 1990. "Colloidal Considerations in Groundwater Sampling and Contaminant Transport Predictions." *Nucl. Safety*, 31(1):58-65.
- Puls, R. W., D. A. Clark, B. Bledsoe, R. M. Powell, and C. J. Paul. 1992. "Metals in Ground Water: Sampling Artifacts and Reproducibility." *Hazardous Waste and Hazardous Materials*, 9(2):149-162.
- Puls, R. W., C. J. Paul, and D. A. Clark. 1993. "Surface Chemical Effects on Colloid Stability and Transport Through Natural Porous Media." *Colloids Surf. A.*, 73, 287-300.
- Relyea, J. F. 1982. "Theoretical and Experimental Considerations for the Use of the Column Method for Determining Retardation Factors." *Radioactive Waste Management and the Nuclear Fuel Cycle*, 3(3):151-166.
- Ronen, D. M., M. Magaritz, U. Weber, A. J. Amiel, and E. Klein. 1992. "Characterization of Suspended Particles Collected in Groundwater Under Natural Gradient Flow Conditions." *Water Resour. Res.*, 28, 1279-1291.
- Ryan, J. N., and M. Elimelech. 1996. "Colloid Mobilization and Transport in Groundwater." *Colloids Surf. A.*, 107:1-56.
- Ryan, J. N., and P. M. Gschwend. 1990. "Colloid Mobilization in Two Atlantic Coastal Plain Aquifers: Field Studies." *Water Resour. Res.* 26:307-322.
- Ryan, J. N., and P. M. Gschwend. 1994. "Effect of Solution Chemistry on Clay Colloid Release from an Iron Oxide-Coated Aquifer Sand." *Environ. Sci. Technol.*, 28(9):1717-1726.
- Schwertmann, U., and R. M. Taylor. 1989. "Iron Oxides." In: *Minerals in Soil Environments, 2nd Edition*, J. B. Dixon, and S. B. Week, Eds., Soil Science Society of America, Madison, Wisconsin.
- Seaman, J. C., P. M. Bertsch, and W. P. Miller. 1995. "Chemical Controls on Colloid Generation and Transport in a Sandy Aquifer." *Environ. Sci. Tech.*, 29(7):1808-1815.
- Sharma, M. M., and Y. C. Yortsos. 1987. "Fines Migration in Porous Media." *Amer. Inst. Chem. Eng. J.*, 33(10):1654-1662.

- Shields, K. D. 1995. *Comparison of Soil Physical Properties for Carbon Tetrachloride and Water Using the UFA Method*, Master of Science Thesis, Washington State University, Pullman, Washington.
- Spielman, L.A., and S.L. Goren. 1970. "Capture of Small Particles by London Forces from Low-Speed Liquid Flows." *Environ. Sci. Technol.* 4:135-140.
- Suarez, D.L., F. K. Rhoades, R. Lavado, and D. M. Grieve. 1984. "Effect of pH on Saturated Hydraulic Conductivity and Soil Dispersion." *Soil Sci. Soc. Am. J.*, 48:50-55.
- Tien, C. 1989. *Granular Filtration of Aerosols and Hydrosols*. Butterworth Publishers, Boston.
- Travis, B. J., and J. E. Nuttal. 1985. "A Transport Code for Radiocolloid Migration: With an Assessment of an Actual Low-Level Waste Site." In: *Scientific Basis for Nuclear Waste Management VIII*, C. M. Jantzen, J. A. Stone, and R. C. Ewing, Eds., Materials Research Society, Pittsburgh, 969-976.
- van Genuchten, M. T. 1980. "A Closed Form Equation for Predicting the Hydraulic Conductivity of Unsaturated Soils." *Soil Sci. Soc. Am. J.*, 44:892-898.
- van Olphen, H. 1977. *An Introduction to Clay Colloid Chemistry*. 2nd Edition. Wiley-Interscience, New York.
- Wan, J., and J. L. Wilson. 1994a. "Visualization of the Role of the Gas Water Interface on the Fate and Transport of Colloids in Porous Media." *Water Resour. Res.*, 30(1):11-23.
- Wan, J., and J. L. Wilson. 1994b. "Colloid Transport in Unsaturated Porous Media." *Water Resour. Res.*, 30(4):857-864.
- Wood, W. W., and M. J. Petraitis. 1984. "Origin and Distribution of Carbon Dioxide in the Unsaturated Zone of the Southern High Plains of Texas." *Water Resour. Res.*, 20(9):1193-1208.
- Yao, K., M.T. Habibian, and C.R. O'Melia. 1971. "Water and Waste Water Filtration: Concepts and Applications." *Environ. Sci. Technol.* 5:1105-1112.
- Zar, J. H. 1974. *Biostatistical Analysis*, Prentice-Hall, Inc., Englewood Cliffs, New Jersey.

Appendix A

Fluorescent Emission Scans and Calibration Curves for Latex Colloids

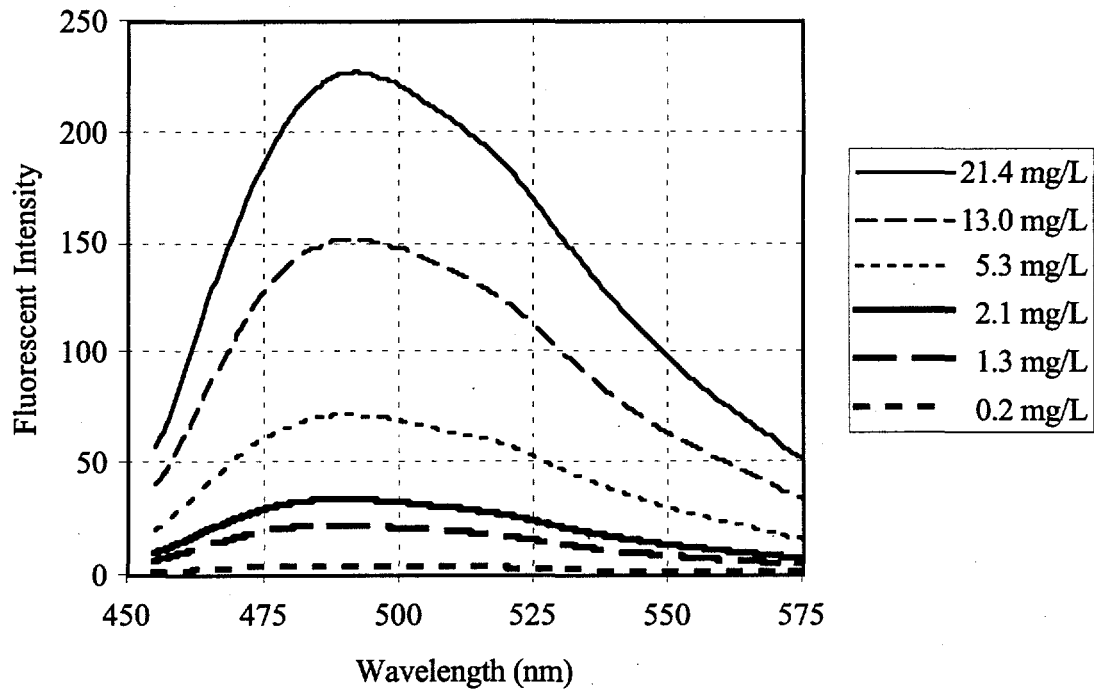


Figure A.1. Emission Spectra of the 52-nm Colloids at Different Concentrations

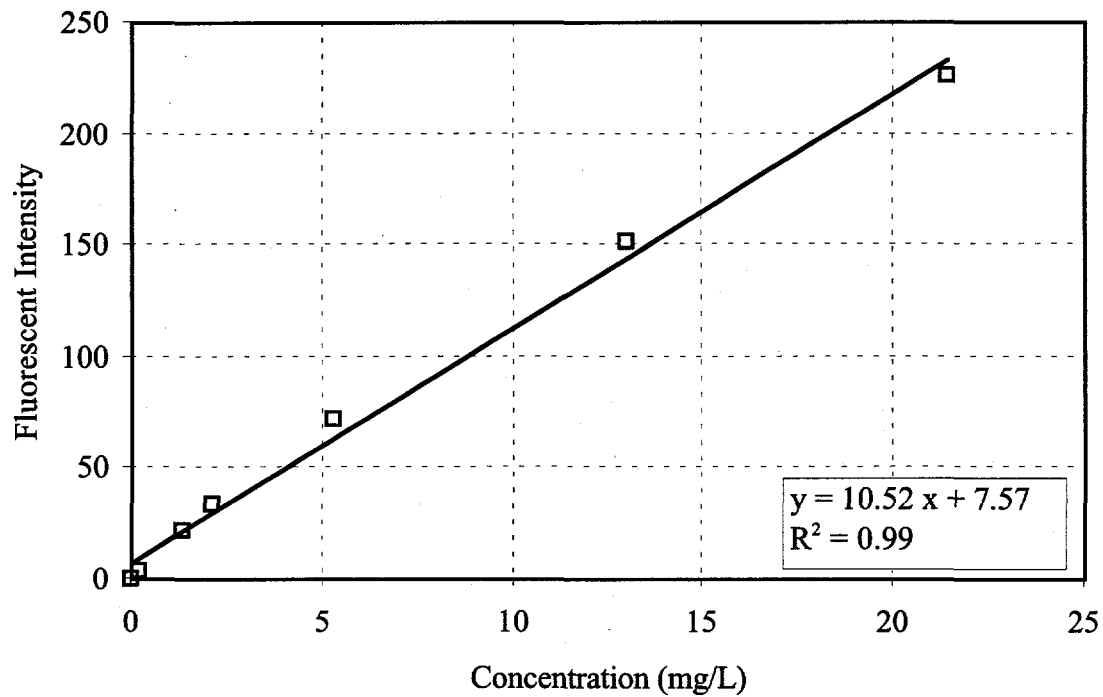


Figure A.2. Calibration Curve for the 52-nm Colloids (Ex = 440 nm, Em = 489 nm)

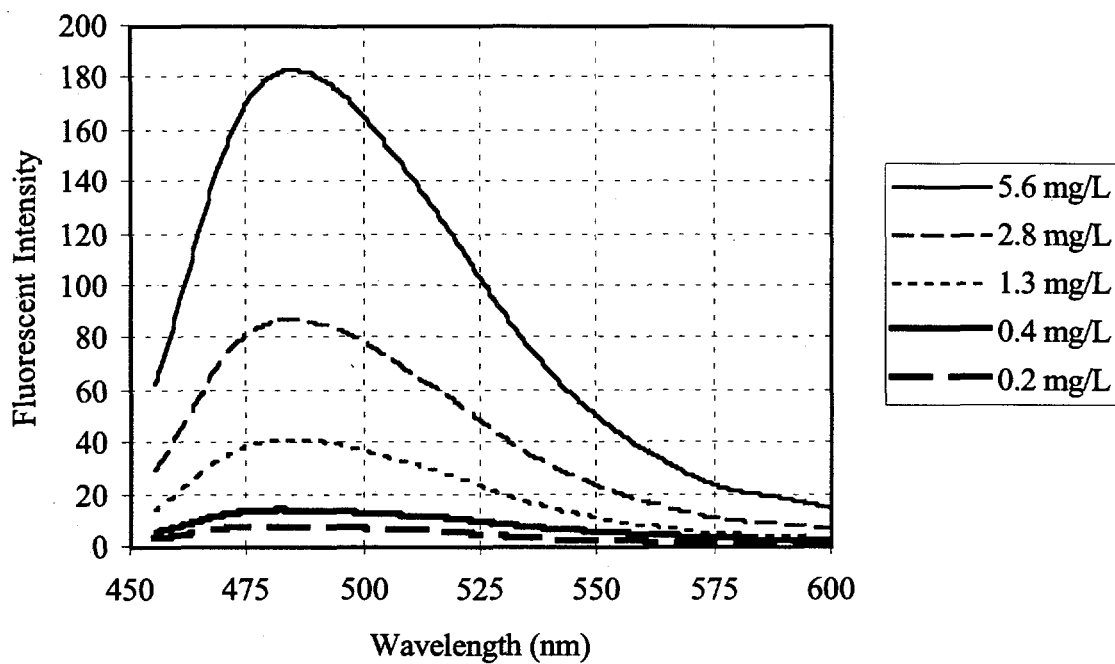


Figure A.3. First Emission Spectra of the 545-nm Colloids at Different Concentrations

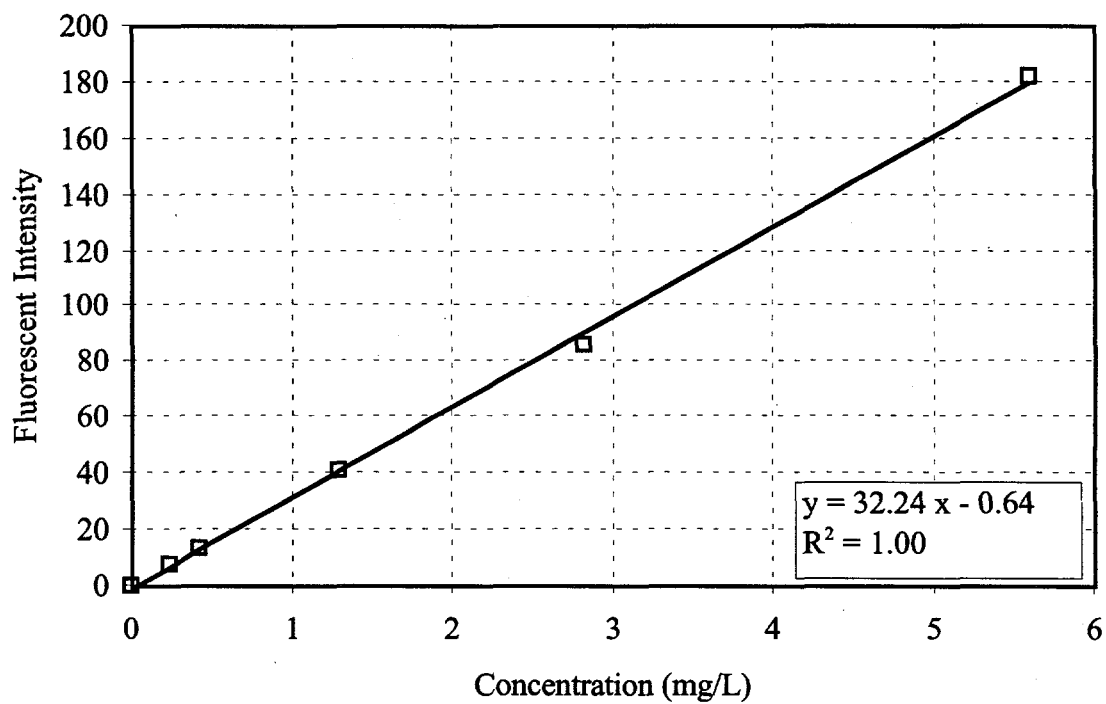


Figure A.4. First Calibration Curve for the 545-nm Colloids (Ex = 440 nm, Em = 485 nm)

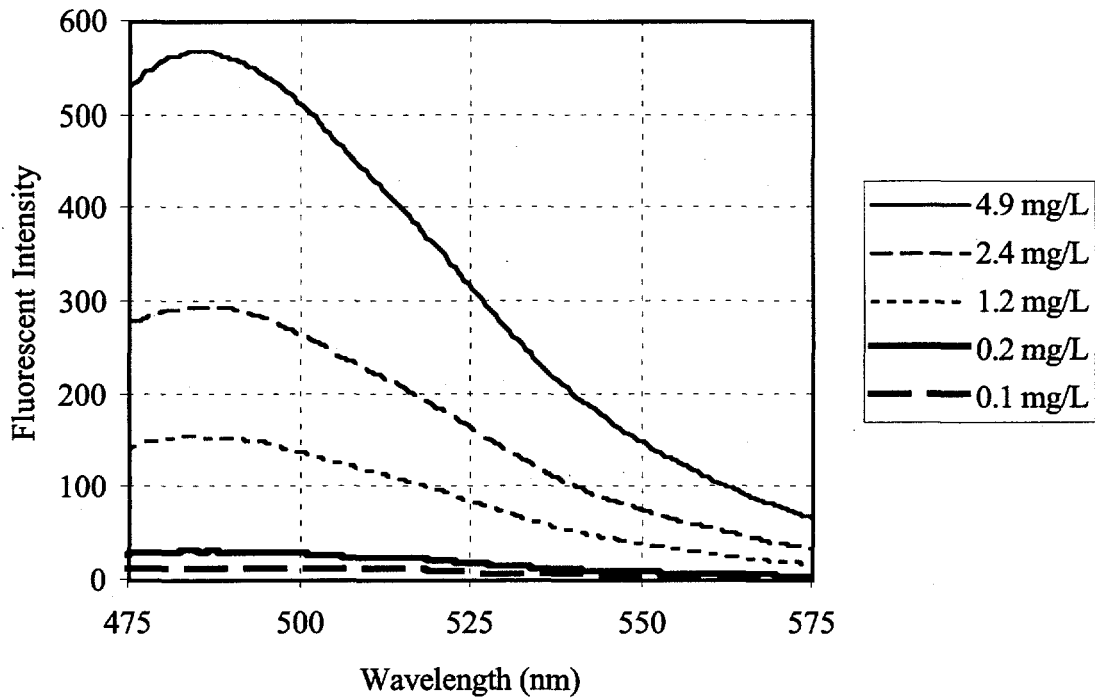


Figure A.5. Emission Spectra of the 545-nm Colloids at Different Concentrations After Maintenance

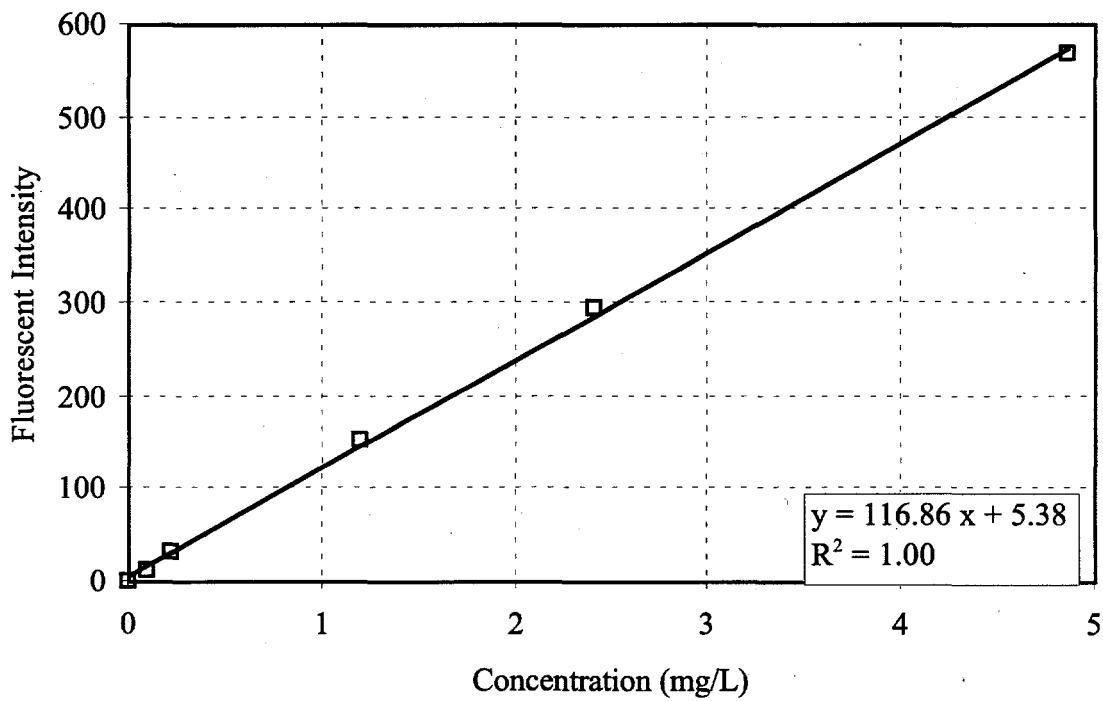


Figure A.6. Calibration Curve for the 545-nm Colloids After Maintenance (Ex = 440 nm, Em = 485 nm)

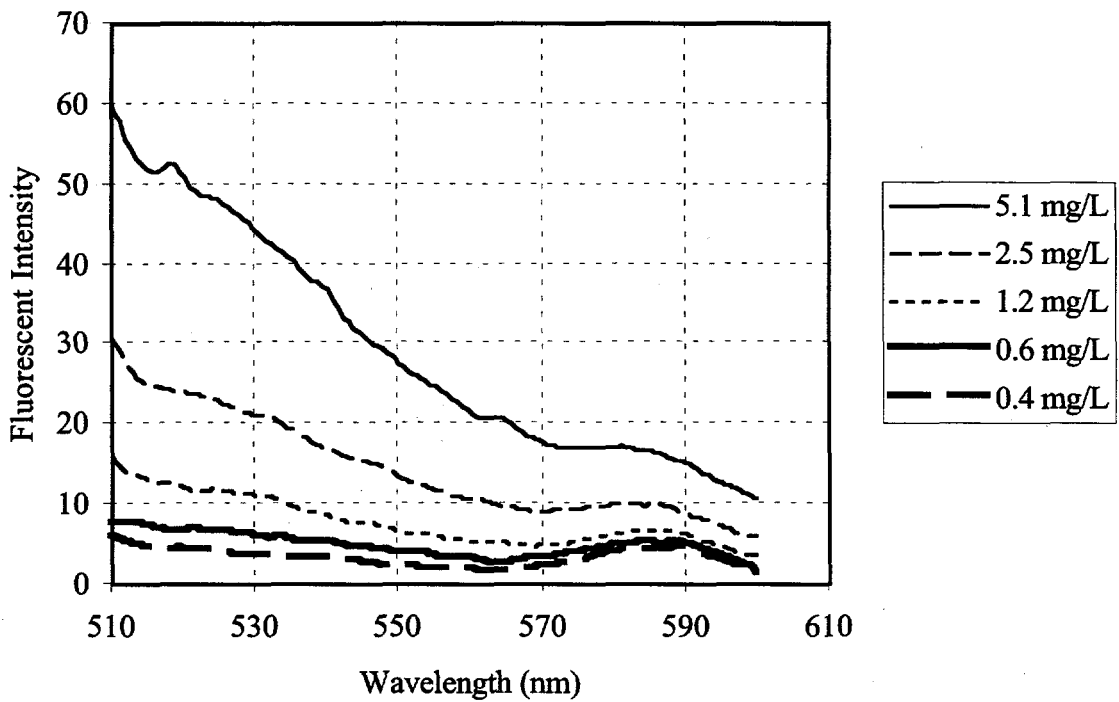


Figure A.7. Emission Spectra of the 910-nm Colloids at Different Concentrations

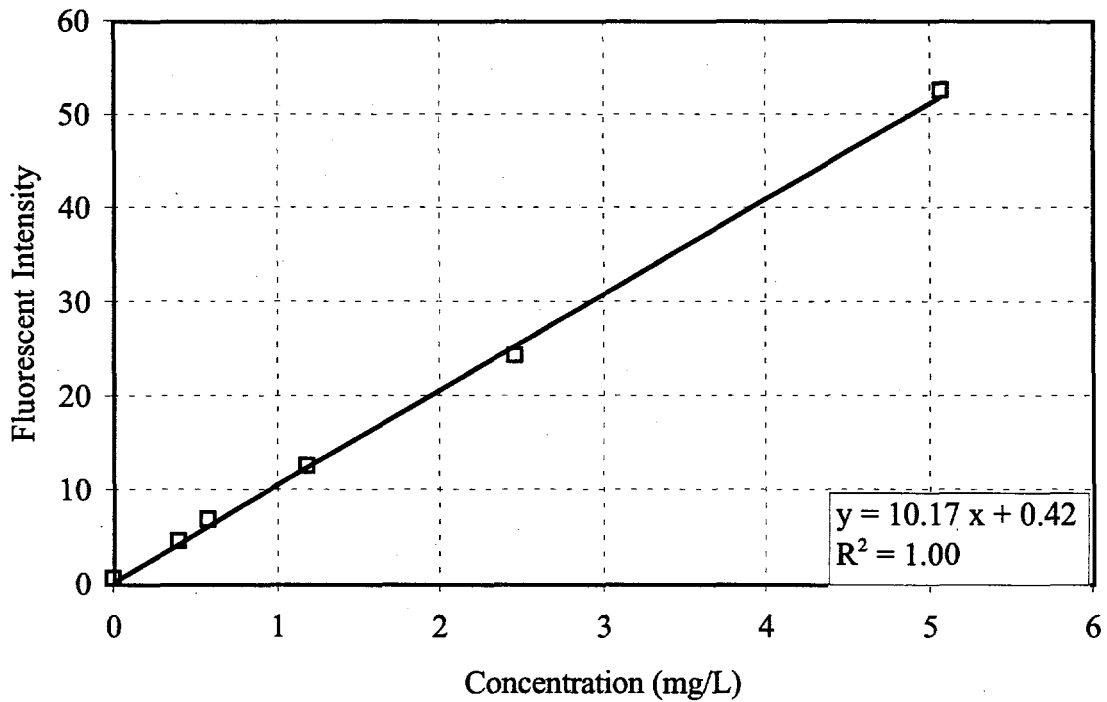


Figure A.8. Calibration Curve for the 910-nm Colloids (Ex = 490 nm, Em = 518 nm)

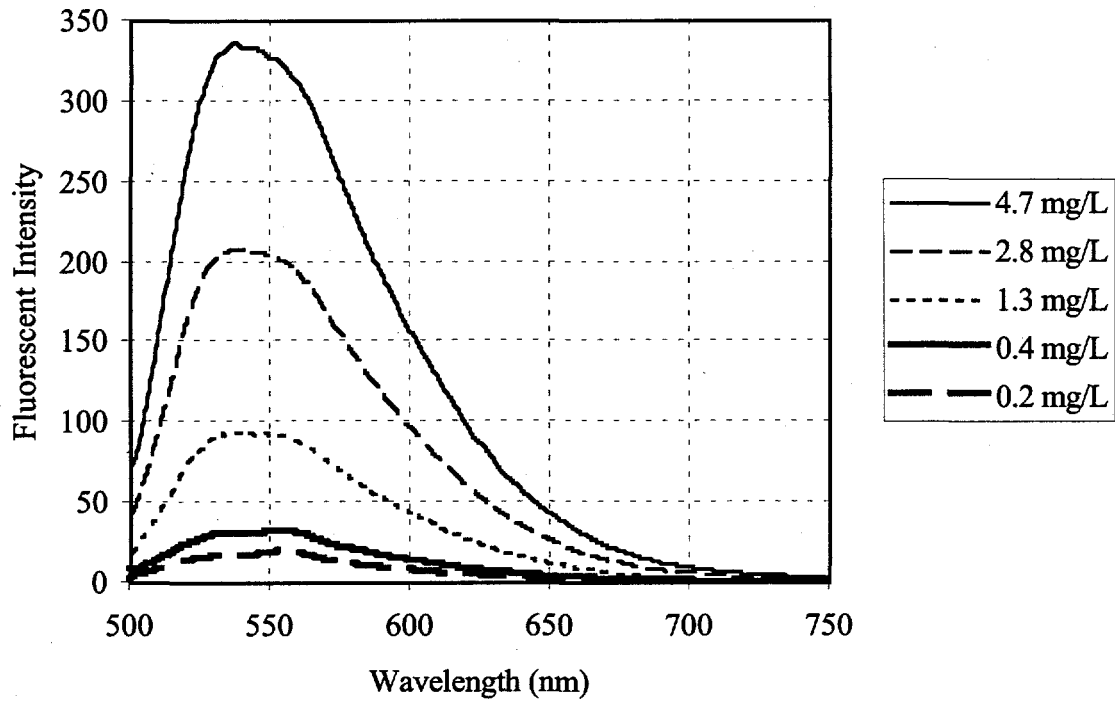


Figure A.9. Emission Spectra of the 1900-nm Colloids at Different Concentrations

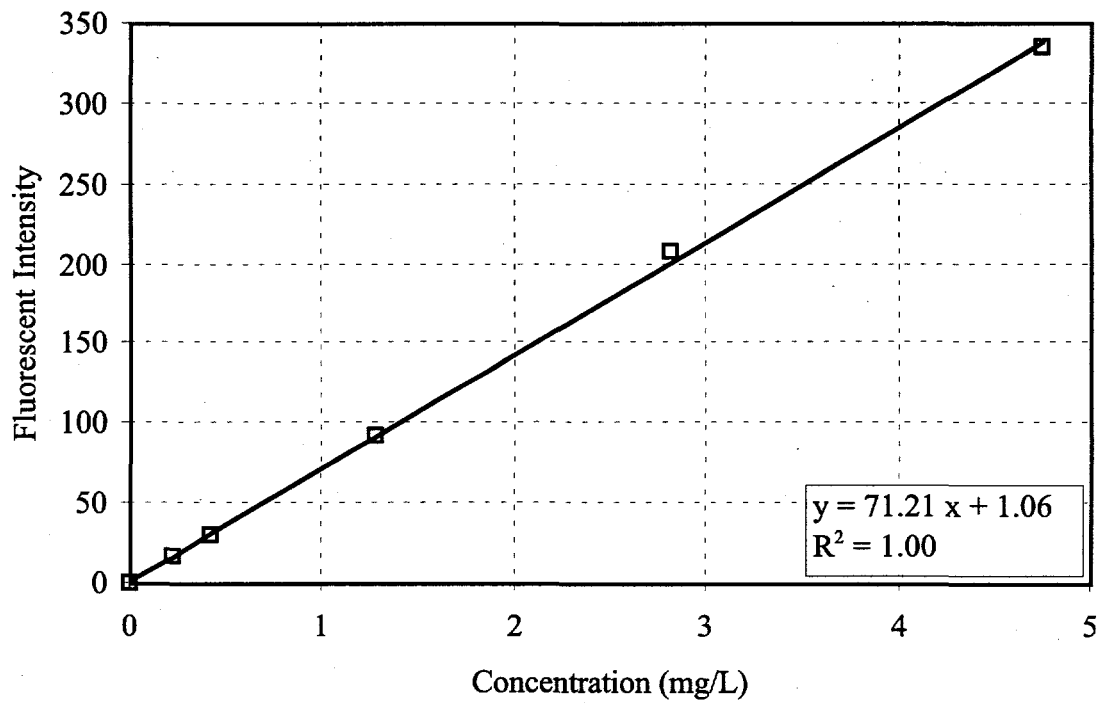


Figure A.10. Calibration Curve for the 1900-nm Colloids (Ex = 468 nm, Em = 536 nm)

Appendix B

Average Volumetric Water Content

Table B.1. Averaged Volumetric Water Content, Hydraulic Conductivity, and Standard Deviations. The data were used to plot Figure 4.10.

Number of samples	Average volumetric water content	Average hydraulic conductivity (cm/s)	Maximum hydraulic conductivity (cm/s)	Minimum hydraulic conductivity (cm/s)
4	1.78 ± 0.24	3.13 x 10 ⁻⁰⁸ ± 7.28 x 10 ⁻¹²	3.13 x 10 ⁻⁰⁸	1.09 x 10 ⁻¹¹
4	2.64 ± 0.24	9.72 x 10 ⁻⁰⁷ ± 1.57 x 10 ⁻⁰⁶	3.31 x 10 ⁻⁰⁶	8.28 x 10 ⁻⁰⁸
4	3.31 ± 0.19	2.56 x 10 ⁻⁰⁶ ± 3.22 x 10 ⁻⁰⁶	7.36 x 10 ⁻⁰⁶	4.14 x 10 ⁻⁰⁷
15	4.61 ± 0.32	6.82 x 10 ⁻⁰⁶ ± 1.43 x 10 ⁻⁰⁶	7.36 x 10 ⁻⁰⁶	3.31 x 10 ⁻⁰⁶
15	5.43 ± 0.22	9.21 x 10 ⁻⁰⁶ ± 3.83 x 10 ⁻⁰⁶	1.66 x 10 ⁻⁰⁵	7.36 x 10 ⁻⁰⁶
7	6.44 ± 0.35	9.42 x 10 ⁻⁰⁶ ± 5.12 x 10 ⁻⁰⁶	1.66 x 10 ⁻⁰⁵	3.31 x 10 ⁻⁰⁶
2	8.66 ± 1.50	1.20 x 10 ⁻⁰⁵ ± 6.53 x 10 ⁻⁰⁶	1.66 x 10 ⁻⁰⁵	7.36 x 10 ⁻⁰⁶
2	10.67 ± 0.13	1.20 x 10 ⁻⁰⁵ ± 6.53 x 10 ⁻⁰⁶	1.66 x 10 ⁻⁰⁵	7.36 x 10 ⁻⁰⁶
3	11.71 ± 0.25	4.13 x 10 ⁻⁰⁵ ± 5.10 x 10 ⁻⁰⁵	1.00 x 10 ⁻⁰⁴	7.36 x 10 ⁻⁰⁶
2	16.29 ± 0.39	1.00 x 10 ⁻⁰⁴ ± 0.00 x 10 ⁻⁰⁰	1.00 x 10 ⁻⁰⁴	1.00 x 10 ⁻⁰⁴
4	20.03 ± 0.63	1.00 x 10 ⁻⁰⁴ ± 0.00 x 10 ⁻⁰⁰	1.00 x 10 ⁻⁰⁴	1.00 x 10 ⁻⁰⁴
3	22.46 ± 1.13	8.20 x 10 ⁻⁰⁵ ± 3.12 x 10 ⁻⁰⁵	1.00 x 10 ⁻⁰⁴	4.60 x 10 ⁻⁰⁵
2	25.67 ± 0.36	1.15 x 10 ⁻⁰⁴ ± 9.75 x 10 ⁻⁰⁵	1.84 x 10 ⁻⁰⁴	4.60 x 10 ⁻⁰⁵
2	29.30 ± 0.93	1.42 x 10 ⁻⁰⁴ ± 5.94 x 10 ⁻⁰⁵	1.84 x 10 ⁻⁰⁴	1.00 x 10 ⁻⁰⁴
14	36.14 ± 1.52	2.46 x 10 ⁻⁰³ ± 1.44 x 10 ⁻⁰³	5.51 x 10 ⁻⁰³	1.32 x 10 ⁻⁰⁴
16	38.27 ± 2.21	3.57 x 10 ⁻⁰³ ± 2.19 x 10 ⁻⁰³	7.53 x 10 ⁻⁰³	9.86 x 10 ⁻⁰⁴
2	40.16 ± 2.68	3.95 x 10 ⁻⁰³ ± 5.27 x 10 ⁻⁰⁴	4.32 x 10 ⁻⁰³	3.57 x 10 ⁻⁰³

Distribution

No. of Copies			No. of Copies
OFFSITE			2 Lockheed Martin Hanford Company
2	DOE/Office of Scientific and Technical Information		R. J. Murkowski H5-03 J. A. Voogd H5-03
ONSITE			15 Pacific Northwest National Laboratory
3	DOE Richland Operations Office		M. J. Fayer K9-33 D. I. Kaplan (5) K6-81 C. T. Kincaid K9-33 B. P. McGrail K6-81 E. M. Murphy K3-61 R. J. Serne K6-81 Information Release (5) K1-06
	N. R. Brown K6-51 D. D. Button K6-51 P. E. Lamont S7-53		
2	Fluor Daniel Northwest		
	F. M. Mann H0-31 R. Khaleel H0-31		1 Rust Federal Services Hanford M. I. Wood H6-06